www.sciencemag.org/cgi/content/full/science.aaa9804/DC1

Supplementary Materials for

Effect of the cytoplasmic domain on antigenic characteristics of HIV-1 envelope glycoprotein

Jia Chen, James M. Kovacs, Hanqin Peng, Sophia Rits-Volloch, Jianming Lu, Donghyun Park, Elise Zablowsky, Michael S. Seaman, Bing Chen*

*Corresponding author. E-mail: bchen@crystal.harvard.edu

Published 25 June 2015 on *Science* Express
DOI: 10.1126/science.aaa9804

This PDF file includes:

Materials and Methods

Generation of 293T cell lines stably transfected with HIV-1 Env constructs

The expression construct of HIV-1 92UG037.8 gp160 was synthesized by GenScript (Piscataway, NJ). The C97ZA012 gp160 plasmid used in this study was kindly provided by John Mascola (VRC, NIH). Constructs, gp160ΔCT, gp160ΔCT-nonHis, gp160-CT30, gp160-CT60, gp160-CT90 and gp160-CT120, gp140-GPI, gp140-TM-fd, gp140-FL20-TM, gp140-FL20-TM-fd and C97ZA012 gp160ΔCT were generated by standard PCR-based protocols and cloned into pCMV-IRES-puro vector (Codex BioSolutions, Inc, Gaithersburg, MD) for generation of stable cell lines. All truncations and mutations were confirmed by DNA sequencing. The 293T cell lines stably transfected with these envelope constructs were generated either in-house or at Codex Biosolutions. Briefly, $8x10^5$ HEK-293T cells in 2 ml of DMEM containing 10% FBS and no antibiotics were seeded on a 6 well-plate and incubated for overnight. The cells were then transfected with an Env construct in the pCMV-IRES-puro expression vector using Lipofectamine 3000 (Life Technologies, Grand Island, NY) following a protocol recommended by manufacturer. 24 hours post-transfection, the transfected cells were transferred into a medium containing DMEM, 10% FBS and 1 μg/ml puromycin for selection. Single colonies were picked in 2-3 weeks, and transferred into 24-well plates in the same selective medium. Expression of HIV-1 Env was confirmed by both western blot and a fluorescence-activated cell sorting (FACS) assay (see below). Positive clones were expanded, frozen and stored at -80°C.

Production of antibodies, Fab fragments and peptides

We have generated expression constructs of antibodies 2G12, PG9, PG16, PGT145, PGT128, 2F5, 4E10, 10E8, 412d using synthetic genes made by GeneArt Gene Synthesis (Life Technologies) or GenScript. The VRC01 and PGV04 expression constructs were kindly provided by John Mascola (VRC, NIH); the expression constructs of NIH45-46, 12A12, 8ANC195, 10-1074, 3BC176, 1NC9, 3BNC176 by Michel Nussenzweig (Rockefeller University), the constructs of CH01 by Barton Haynes (Duke University), the constructs of PGT151 and PGT152 by Dennis Burton and Pascal Poignard (Scripps);

the CHO stable line expressing antibody b6 by Dennis Burton (Scripps); 17b, A32, 7b2, 19b hybridomas by James Robinson (Tulane University); 2158, 3791, 240-D, 246-D, 1281, 167-D hybridomas by Susan Zolla-Pazner (New York University). The expression constructs of 10E8 and 35O22 were obtained from the NIH AIDS reagent program (10E8 heavy chain (Cat# 12290) and 10E8 light chain (Cat# 12291); 35O22 heavy chain (Cat# 12584) and 35O22 light chain (Cat# 12585)). The intact antibodies or Fab fragments were expressed in 293T cells either by transient transfection or using selected stably transfected clones, or from hybridomas or CHO cells. The antibodies were purified by affinity chromatography using Gamma bind plus resin (GE Healthcare, Pittsburgh, PA), followed by gel-filtration chromatography. Fab preparations by papain digestion were carried out as described (*34*). HR2 (heptad repeat 2; Fig. S1) derived peptides used in this study include a histagged T20 (HHHHHHHHYTSLIHSLIEESQNQQEKNEQELLELDKWASLWNWF), C34 (WMEWDREINNYTSLIHSLIEESQNQQEKNEQELL) and biotin-C38 (bio-WMEWDREINNYTSLIHSLIEESQNQQEKNEQELLELDK). T20 and C34 were synthesized by Tufts University Core Facility (Boston, MA) and biotin-C38 was synthesized in-house using FMOC chemistry on PAL (PE Biosystems, Warrington U.K.) supports using Applied Biosystems model 431 peptide synthesizer.

Immunoprecipitation and western blot

Whole cell lysates were prepared by resuspending the cells in PBS (phosphate buffered saline) at a density of $2x10^6$ cells/ml, followed by treatment with Laemmli Sample Buffer (Bio-Rad, Hercules, CA) and boiling for 5 minutes. To prepare cell membrane fractions, frozen cell pellets were thawed in a low salt buffer containing 10 mM HEPES, pH 7.5, 10 mM $MgCl_2$, 20 mM KCl, and EDTA-free complete protease inhibitor cocktail (Roche), and washed with the same buffer. The cells were then treated by a hypertonic solution containing the low salt buffer with addition of 1M NaCl and the cell membrane fractions were pelleted by centrifugation. The pellets were repeatedly washed by the hypertonic solution, followed by a final wash in PBS or 25 mM Tris, pH7.5 and 150 mM NaCl to remove the high salt. To prepare the cell-surface Env samples by immunoprecipitation, Env-expressing cells were incubated with either VRC01 or PGT128 on ice for 30 minutes

and washed by PBS three times. The cell pellets were resuspended in an ice-cold Pierce IP Lysis Buffer (Thermo Scientific, Waltham, MA) containing protease inhibitors, and then incubated on ice for 5-10 minutes with periodic mixing. Cell debris was removed by centrifugation at 18,000 xg for 10 minutes at 4°C. The supernatant was then mixed with Capture Select CH1 beads (Life Technologies) and incubated at room temperature for additional 30 minutes. The beads were washed with PBS containing 0.2% NP-40, and boiled in the Bio-Rad Laemmli Sample Buffer for 5 minutes.

For western blot, Env samples were resolved in 4-15% Mini-Protean TGX gel (Bio-Rad) and transferred onto PVDF membranes (Millipore, Billerica, MA) by an Iblot2 (Life Technologies). Membranes were blocked with 5% skimmed milk in PBS for 1 hour and incubated with anti-V3 loop antibody 3791 for another hour at room temperature. Either horseradish peroxidase conjugated anti-human Fab IgG (1:25000) (Sigma-Aldrich, St. Louis, MO) or alkaline phosphatase conjugated anti-human Fab IgG (1:5000) (Sigma-Aldrich) was used as a secondary antibody. Env proteins were visualized using either Western Bright ECL (Advansta, Menlo Park, CA) or one-step NBT/BCIP substrates (Thermo Scientific).

Flow cytometry

To obtain high-quality, reproducible antibody binding data using HIV-1 Env expressed on cell surfaces by a fluorescence-activated cell sorting (FACS) assay, it was necessary to produce stable 293T cell lines expressing constant levels of various HIV-1 Env constructs. Env-expressing cells were detached from cell flasks using PBS, and washed with ice-cold PBS containing 1% BSA. 10^6 cells were incubated for 30~40 minutes either on ice or at 37ºC with anti-Env monoclonal antibodies at concentrations of 0.005-50 μg/ml in PBS containing 1% BSA, either in the absence or presence of soluble CD4 at a concentration of 3 μM. CD4 was preincubated with the cells for 10 minutes before addition of an antibody. The cells were then washed twice with PBS containing 1% BSA and stained with R-Phycoerythrin AffiniPure $F(ab')_2$ fragment goat anti-human IgG, $F(ab')_2$ Fragment specific secondary antibody (Jackson ImmunoResearch laboratories, West Grove, PA) at 5 μg/ml. Bound CD4 was also detected by an Anti-His antibody

conjugated to fluoresceinisothiocyanate (FITC) (Miltenyi Biotec Inc., San Diego, CA). To detect the prehairpin intermediate conformation of gp41, a biotinylated, HR-2 derived peptide biotin-C38 was used for gp41 binding, and subsequently detected by Brilliant Violet 421 Streptavidin (BioLegend, San Diego, CA). All the fluorescently labeled cells were washed twice with PBS containing 1% BSA and analyzed immediately using a BD LSRII instrument and program FACSDIVA (BD Biosciences, Franklin Lakes, New Jersey). Extensive control experiments were carried out to ensure the binding specificity and all experiments were repeated at least two times with almost identical results. All data were analyzed by FlowJo (FlowJo, LLC, Ashland, OR) and plotted in Excel (Microsoft, Redmond, WA) or Cytobank (Cytobank Inc, Mountain View, CA). The Fig. 3 was generated by MatLab (MathWorks, Inc., Natick, MA).

Antibody neutralization assay

Neutralizing IC_{50} values of purified monoclonal antibodies against HIV-1 92UG037.8 and C97ZA012.29 pseudoviruses were measured using a luciferase-based virus neutralization assay in TZM.bl cells as previously described (*35*). The assay measures the reduction in luciferase reporter gene expression in TZM-bl cells following a single round of virus infection. The IC_{50} was calculated as the antibody dilution that resulted in a 50% reduction in relative luminescence units compared with the virus control wells after the subtraction of cell control relative luminescence units. Briefly, 3-fold serial dilutions of antibody samples were performed in duplicate (96-well flat bottom plate) in 10% DMEM growth medium (100 µl/well). Virus was added to each well in a volume of 50 µl, and the plates were incubated for 1 hour at 37°C. TZM.bl cells were then added (1×10^4/well in 100 µl volume) in 10% DMEM growth medium containing DEAE-Dextran (Sigma-Aldrich) at a final concentration of 11 µg/ml. Murine leukemia virus (MuLV) negative controls were included in all assays. HIV-1 Env pseudoviruses were prepared as previously described (*36*).

Cell-cell fusion assays

To assess the membrane fusion capacity of various Env constructs, syncytium formation was visually inspected after mixing Env-expressing cells and TZM-bl cells. Briefly,

$5x10^3$, $2.5x10^4$, $1.5x10^5$ Env-expressing cells were mixed with $1.5x10^5$ TZM-bl cells DMEM medium containing GlutaMax (Life Technologies) and 10% FBS in 24-well plate, either in the absence or presence of T20 peptide at 1 μM. The mixed cells were incubated at 37°C for 10-24 hours and then evaluated for syncytium formation by visual inspection.

To analyze antibody neutralization of modified Env constructs, we have employed another quantitative cell-cell fusion assay based on a reporter gene activation technique described previously (*37*). Briefly, 293T cells were cotransfected by the PEI (polyethylenimine) method with an Env expression construct and a plasmid expressing T7 polymerase; these were designated effector cells. CD4-and CCR5-expressing cells with a luciferase reporter gene under the control of a T7 promotor were designated target cells. The two types of cells were mixed 30 hour posttrasfection, either in absence or presence of a purified antibody at a concentration of 0.5 mg/ml or T20 at 1 μM and then incubated at 37 °C for another 6-12 hr. Fusion activity was measured by a luciferase assay (Promega Assay System and Protocol, E1501; Promega, Madison, WI) following protocols recommended by the manufacturer.

Supplementary Text

Results

We have reported that the MPER-directed bnAbs appear to neutralize by targeting a fusion intermediate of gp41 (*6, 25, 26*), but we have not previously been able to study their properties on intact Env trimers. Because we observed significant CD4-induced gp120 shedding at 37°C by the Env trimers on the cell surfaces (fig. S5C), we chose to test whether the gp41 intermediate state is accessible during the gp120 shedding process. As shown in fig. S28A, an HR2 (heptad repeat 2) derived, biotinylated peptide, biotin-C38 (*38*), only bound the Env trimers at 37°C when they had been triggered by CD4. Its binding signal decreased when the peptide was added 10 min after CD4, and it completely disappeared after 2 hours, suggesting that the transient intermediate conformation of gp41 is indeed detectable during CD4-induced gp120 shedding. Under the same conditions, binding to 2F5, 4E10 and 10E8 was greatly enhanced (up to 13-fold) when CD4 was present, and it increased even further (up to 27-fold) when another HR2-based peptide C34 (*2*) was used to capture the intermediate state (fig. S28B). We did not detect increased binding by VRC01 and 35O22. The binding signal for the MPER antibodies was still weaker than that for VRC01, probably because they detect only the small population of cleaved Env from which gp120 has dissociated. Nonetheless, these data provide the direct evidence, in the context of the full-length, functional Env trimers, that the MPER bnAbs only target a "triggered" form of Env and not the native trimers.

Discussion

There are a number of unexpected findings from our current study which may have far-reaching implications for HIV-1 vaccine development. First, unlike previous reports (*12, 17*), a native Env trimer can indeed adopt a defined and homogenous conformational state with only bnAb epitopes exposed and all non-neutralizing epitopes occluded, without contamination by any irrelevant forms of Env (*12*). This is probably true for all difficult-to-neutralize HIV-1 strains that do not induce autologous neutralizing responses, such as the two described in this work, when the intact cytoplasmic tail is present. This native, untriggered conformation seems to be independent of the cleavage between gp120 and

gp41, since there was a substantial amount of uncleaved gp160 trimer present on cell surfaces that did not bind any of the non-neutralizing antibodies. The Env trimers in this conformation, cleaved or uncleaved, when produced in large quantities, would thus be an ideal immunogen to mimic the native envelope spikes.

Second, it is particularly surprising that the Env cytoplasmic tail has such a large impact on the antigenicity of the ectodomain on the other side of membrane. Various gp160-ΔCT constructs, often with an increased yield, are still widely considered to be faithful substitutes for the full-length gp160, despite published evidence suggesting that the cytoplasmic tail may influence epitope exposure (*31*). Our results unambiguously demonstrate a role for the cytoplasmic tail in preserving the antigenic characteristics of the native Env trimer even in the absence of the matrix protein. In contrast, the Env membrane fusion capacity is not affected significantly by deletion of the cytoplasmic tail. Thus, a “functional” Env may not have a fully “native” antigenic surface (defined by neutralization), as even a fusion-competent Env trimer can expose non-neutralizing epitopes (fig. 3). Soluble, stable gp140 trimers from 92UG037.8 and C97ZA012 and the SOSIP trimers from BG505 and B41 all have antibody-accessible V3 loops (*14-16, 21*). These trimers are not incorrectly folded; rather, we suggest that they represent states in the ensemble of conformations that membrane-anchored gp160 can adopt. Deletion of the cytoplasmic domain, as in our gp160-CT constructs, appears to increase the occupancy of those states substantially. If V3 loop exposure is an early event in the transition from an unliganded conformation toward a CD4-bound one, then soluble gp140 and gp160-CT may represent such a partly "open" structure. Indeed, some features of the SOSIP structure (e.g., full accessibility of all three CD4 binding sites, even though CD4 binding induces or stabilizes a substantial conformational rearrangement) are consistent with this possibility, although we note that full-length BG505 SOSIP Env appears to be non-functional even when the disulfide is reduced (*39*).

The cytoplasmic tail facilitates virus assembly by interacting with the matrix protein and mediating incorporation of Env into nascent virus particles. It has been considered not to have a defined structure in the absence of the matrix protein and thus to be dispensable.

Several intracellular trafficking signals have been found in the CT upstream of residue 785 (*40-42*), but they cannot account for the differences in antigenicity between the gp160 and the gp160-CT90 (truncated at residue 794) or gp160-CT120 (truncated at residue 824). Three membrane-interacting segments (lentiviral lytic peptide (LLP)-2, 3 and 1) have been identified, but mutational studies indicate that they have little impact on viral entry (*43, 44*). We propose that the cytoplasmic tail restrains the ectodomain, either by interacting with the membrane or by forming a defined, oligomeric structure (or both). Whatever the mechanism, our results indicate that the cytoplasmic tail can modulate antigenic properties of the Env trimer, probably by restricting its conformational dynamics, and that certain apparently "harmless" modifications, such as deleting the CT -- an approach widely used in various vaccine strategies to enhance Env yield and/or stability -- can have a strong impact on trimer structure, antigenicity, and potentially immunogenicity.

Third, strain-specific neutralizing epitopes, such as the V3 loop and the V1V2 loop, are well protected on the native trimer derived from the hard-to-neutralize strains we have studied, explaining why it is difficult to induce autologous neutralizing antibody responses against such isolates. It is possible that viruses that do induce autologous neutralizing responses may simply have their strain-specific epitopes better exposed, as on the gp160-ΔCT construct described here. Indeed, as proposed in fig. 4, the antigenic properties of gp160 and gp160-ΔCT may represent, respectively, those of the extreme cases of the difficult-to-neutralize primary isolates that cannot induce autologous neutralizing responses and the easy-to-neutralize, laboratory-adapted strains that induce strong autologous responses, while other isolates (of intermediate susceptibility to neutralization) may adopt conformations in between, like those of our partially truncated gp160-CT constructs. A few mutations within the entire gp160 sequence can easily convert one form into another, perhaps even within a single patient, just as primary and laboratory-adapted SHIV or HIV-1 isolates can be interconverted by in vitro and in vivo passages, respectively (*32*, *33*). Interconversion thus allows Envs on a closely related swarm of viruses to sample a much greater dynamic range at a population level than previously appreciated (*17*). In an infected individual, immune pressure might drive any

particular isolate to evolve into one that is difficult-to-neutralize and does not induce autologous neutralizing responses (fig. 4). Such viruses significantly raise the barrier to vaccine development and may represent an important challenge. If so, Env trimers derived from these isolates should be better starting points for designing immunogens that mimic the native viral spikes.

Fourth, not all bnAbs recognize the native, untriggered Env trimer. The MPER-directed antibodies 2F5, 4E10 and 10E8 clearly recognize only the triggered Env trimers, probably the prehairpin intermediate conformation of gp41 after binding to both CD4 and co-receptor. The conformational states targeted by 35O22 and 3BC176 remain unknown, and further investigation will be needed to dissect the neutralization mechanism of these antibodies. Thus, immunogen design based only on bnAb binding could be misleading.

Finally, non-neutralizing antibodies are believed to provide protection by Fc receptor-mediated effector functions such as antibody-dependent cell-mediated cytotoxicity (ADCC) and complement-dependent cytotoxicity (CDC) (reviewed in ref (*45*)). Such antibodies would not be effective against viruses such as 92UG037.8 or C97ZA012, since none of the non-neutralizing epitopes are exposed and there are no nonfunctional Env for them to bind. Exposure of such epitopes induced by CD4 binding could, however, enhance ADCC and CDC. Thus, a combination of soluble CD4 and ADCC antibodies might be more effective than ADCC antibodies alone.

Fig. S1.

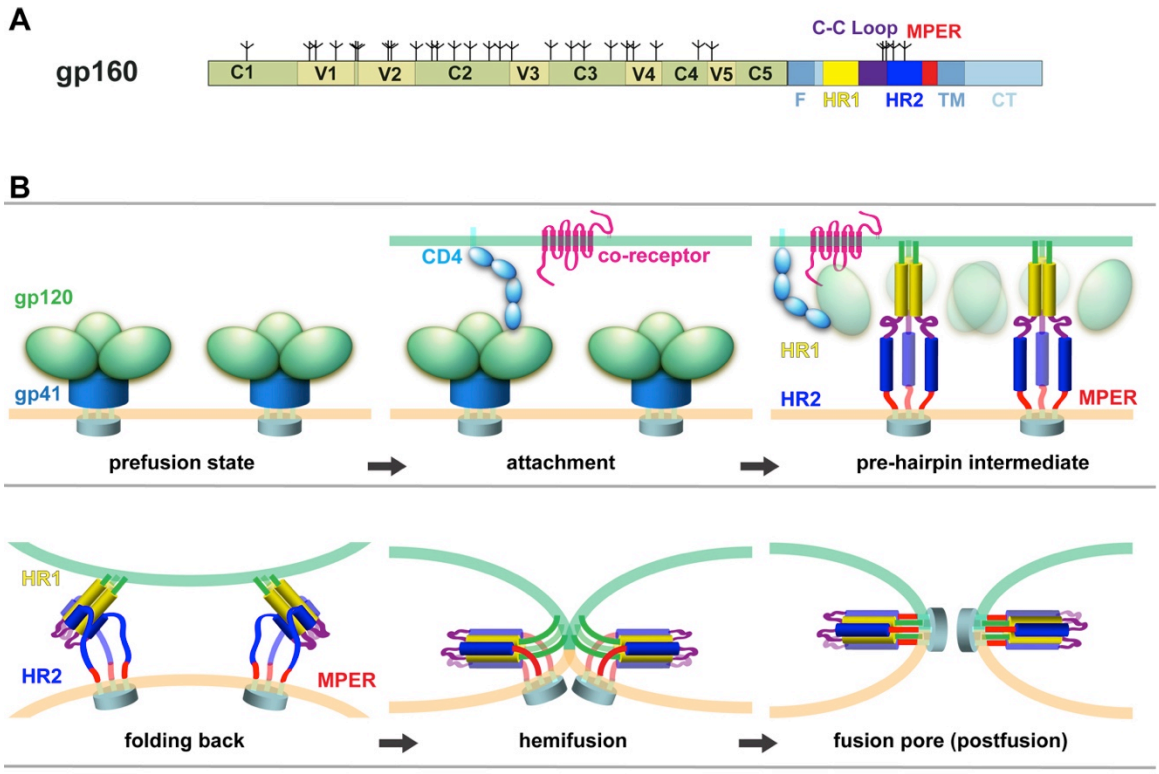

Fig. S1. HIV-1 envelope glycoprotein and viral entry. (**A**) Schematic representation of HIV-1 gp160, the full-length precursor. Segments of gp120 and gp41 are designated as follows: C1-C5, conserved regions 1-5; V1-V5, variable regions 1-5; F, fusion peptide; HR1, heptad repeat 1; C-C loop, the immunodominant loop with a conserved disulfide bond; HR2, heptad repeat 2; MPER, membrane proximal external region; TM, transmembrane anchor; CT, cytoplasmic tail. Tree-like symbols represent glycans. (**B**) Membrane fusion by HIV-1 envelope likely proceeds stepwise as follows. 1) Binding of gp120 (green) to the receptor CD4 (light blue) and coreceptor CXCR4 or CCR5 (magenta) allows viral attachment and triggers structural changes in the envelope glycoprotein. 2) Dissociation of gp120 and insertion of the fusion peptide (green) of gp41 into the target cell membrane leads to the formation of the prehairpin intermediate (*46*). 3) The C-terminal part (HR2 in blue) of gp41 folds back onto the inner core (HR1 in yellow) and brings the two membranes together. 4) A hemifusion stalk forms and resolves into a fusion pore (*47*).

Fig. S2.

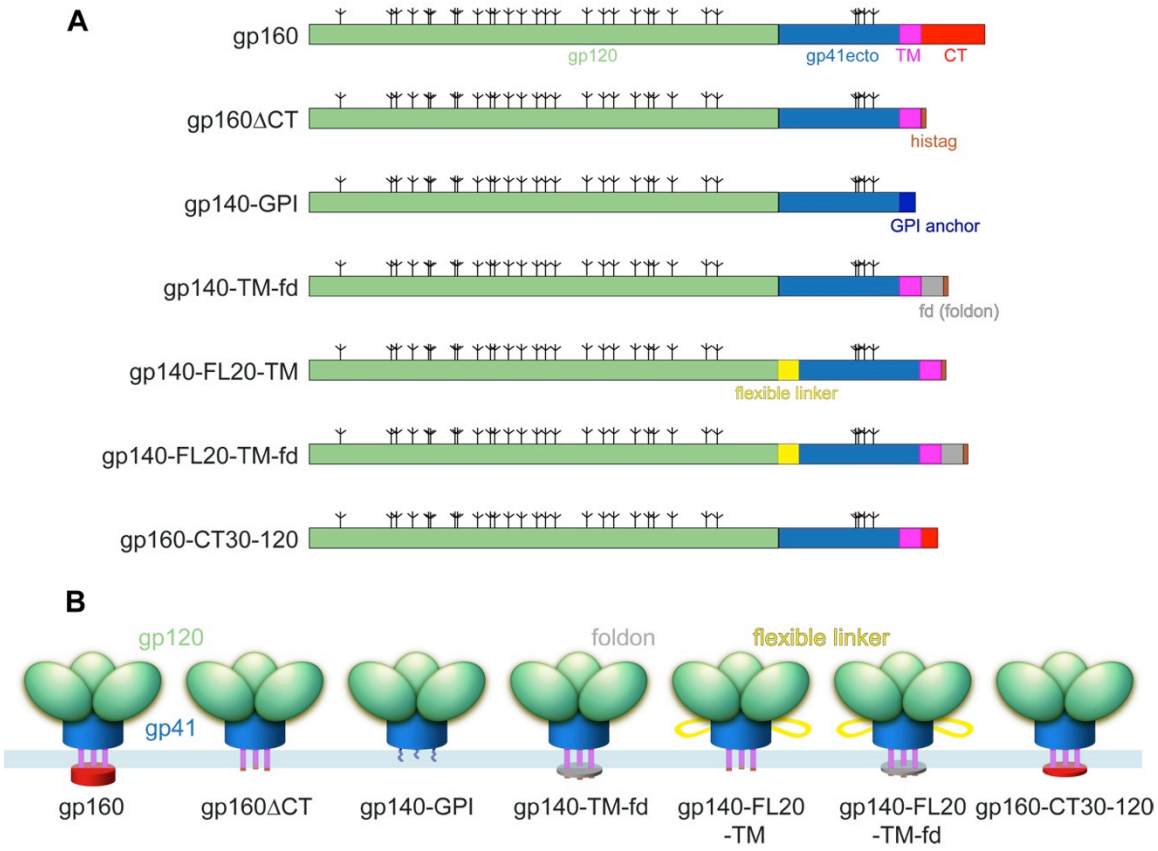

Fig. S2. Design of Env expression constructs. (**A**) Schematic representations of HIV-1 Env constructs: gp160, the full-length precursor containing gp120 (green), gp41 ectodomain (gp41ecto; blue), transmembrane anchor (TM; magenta), cytoplasmic tail (CT; red), and tree-like symbols representing glycans; gp160ΔCT, the gp160 with entire CT deleted and addition of a His-tag (orange) at its C-terminus; gp140-GPI, the ectodomain of gp160 fused with a GPI anchor (dark blue); gp140-TM-fd, the gp160 with the CT replaced with a foldon trimerization tag (fd; gray); gp140-FL20-TM, the gp160ΔCT construct with a 20-residue linker $(SGGGG)_4$ (yellow) inserted between gp120 and gp41; gp140-FL20-TM-fd, the gp140-FL20-TM construct with addition of a foldon tag at its C-terminus; gp160-CT30-120, the gp160 with the serial deletions of CT including four different constructs, gp160-CT30, gp160-CT60, gp160-CT90 and gp160-CT120. Constructs with a name starting with gp160 are functional and those with gp140 are nonfunctional in cell-cell fusion assays. (**B**) Diagrams represent 3-D organizations of each Env trimer. All the segments are shown in the same color scheme as in A.

Fig. S3.

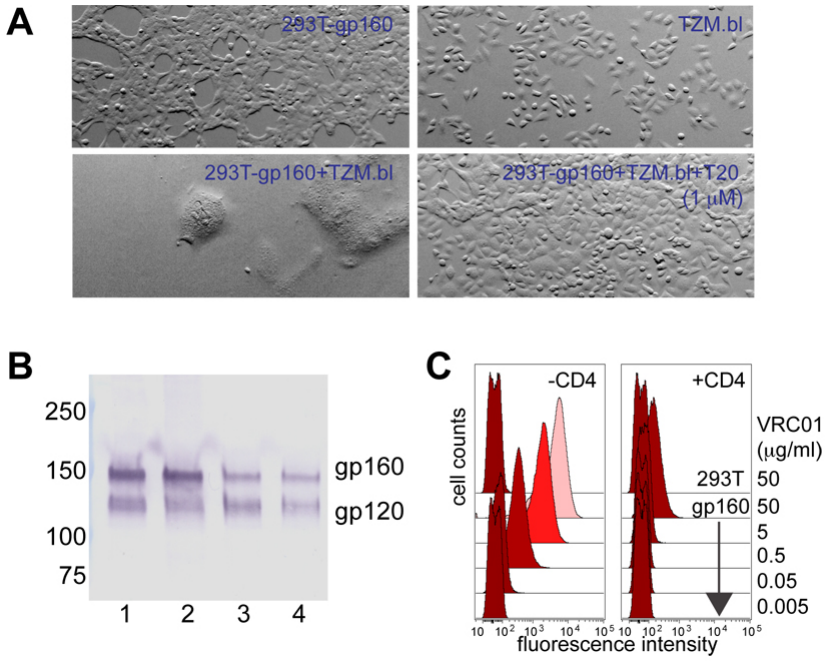

Fig. S3. Characterization of the 92UG037.8 Env trimer presented on cell surfaces. (**A**) 92UG037.8 Env mediated cell-cell fusion. 293T cells stably transfected with 92UG037.8 gp160 (293T-gp160) were mixed with TZM-bl cells in the absence or presence of the fusion inhibitor T20. (**B**) Env samples prepared from the 92UG037.8 gp160 stable cell line are detected by a V3 antibody 3791. Lane1, total cell lysate; lane 2, membrane fraction of the cell; lane 3 and 4, Env trimers on the cell surfaces immuneprecipitated by antibody VRC01 and PGT128, respectively. (**C**) Flow cytometry histograms of VRC01 binding to the Env trimer on the 92UG037.8 gp160 cell surfaces in the absence or presence of soluble CD4. VRC01 concentration varies from 0.005 to 50 μg/ml. VRC01 binding at 50 μg/ml to 293T cells is a negative control.

Fig. S4.

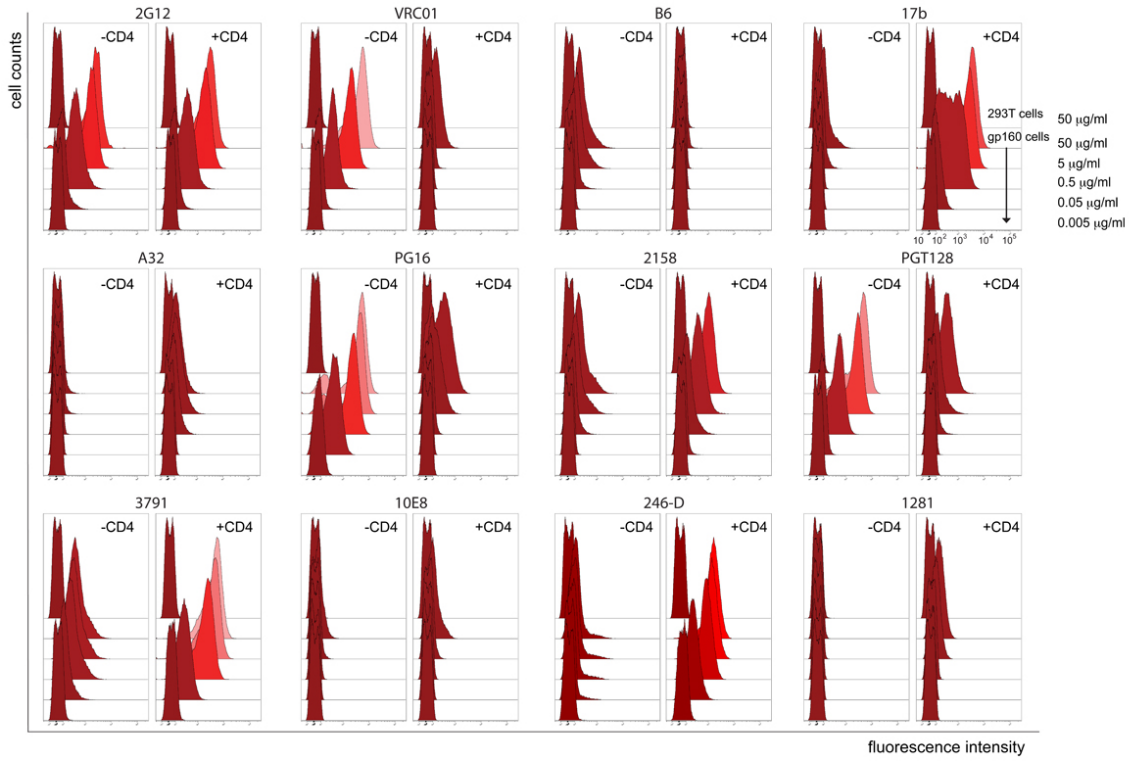

Fig. S4. Flow cytometry histograms of antibody binding to the Env trimer on the 92UG037.8 gp160 cell surfaces by a FACS assay. Data are summarized in fig. 1.

Fig. S5.

A (Fig. S5A)

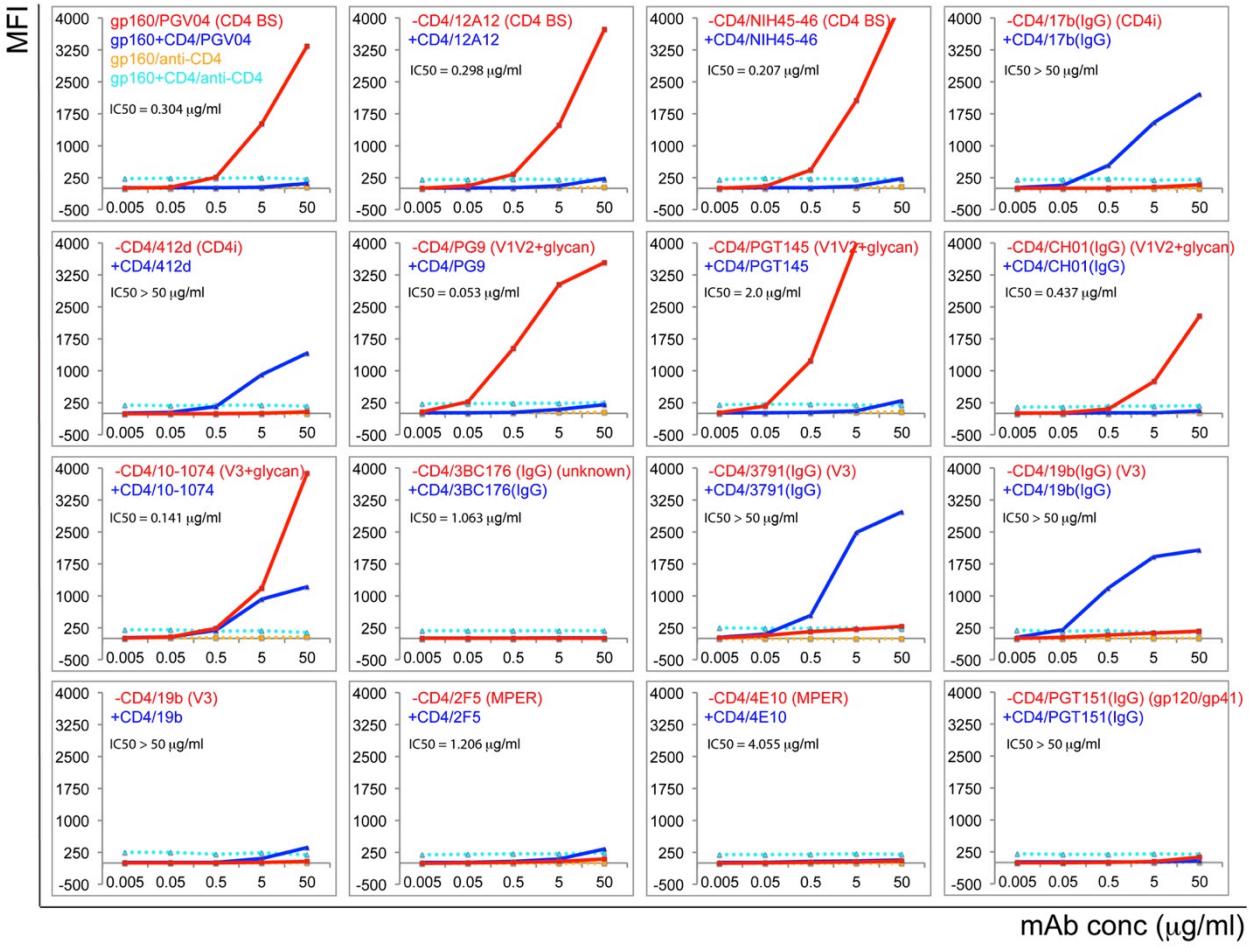

A (Fig. S5A) continued

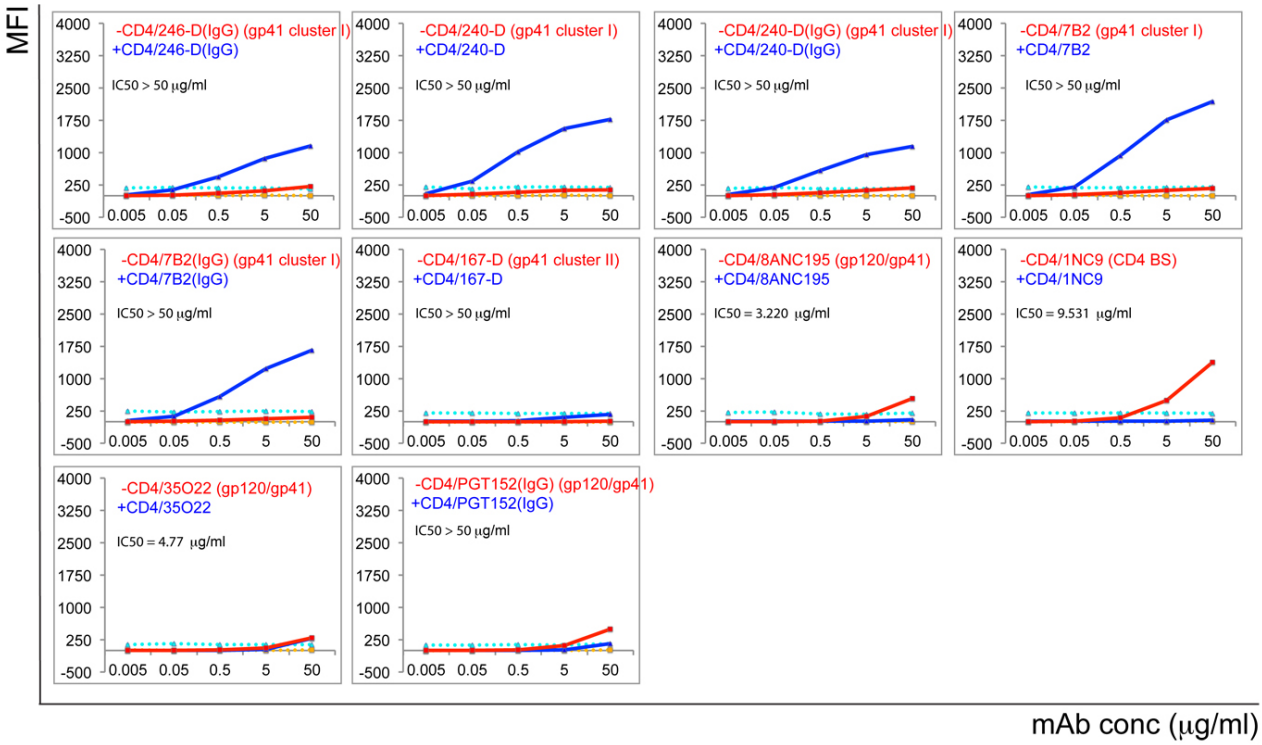

B (Fig. S5B)

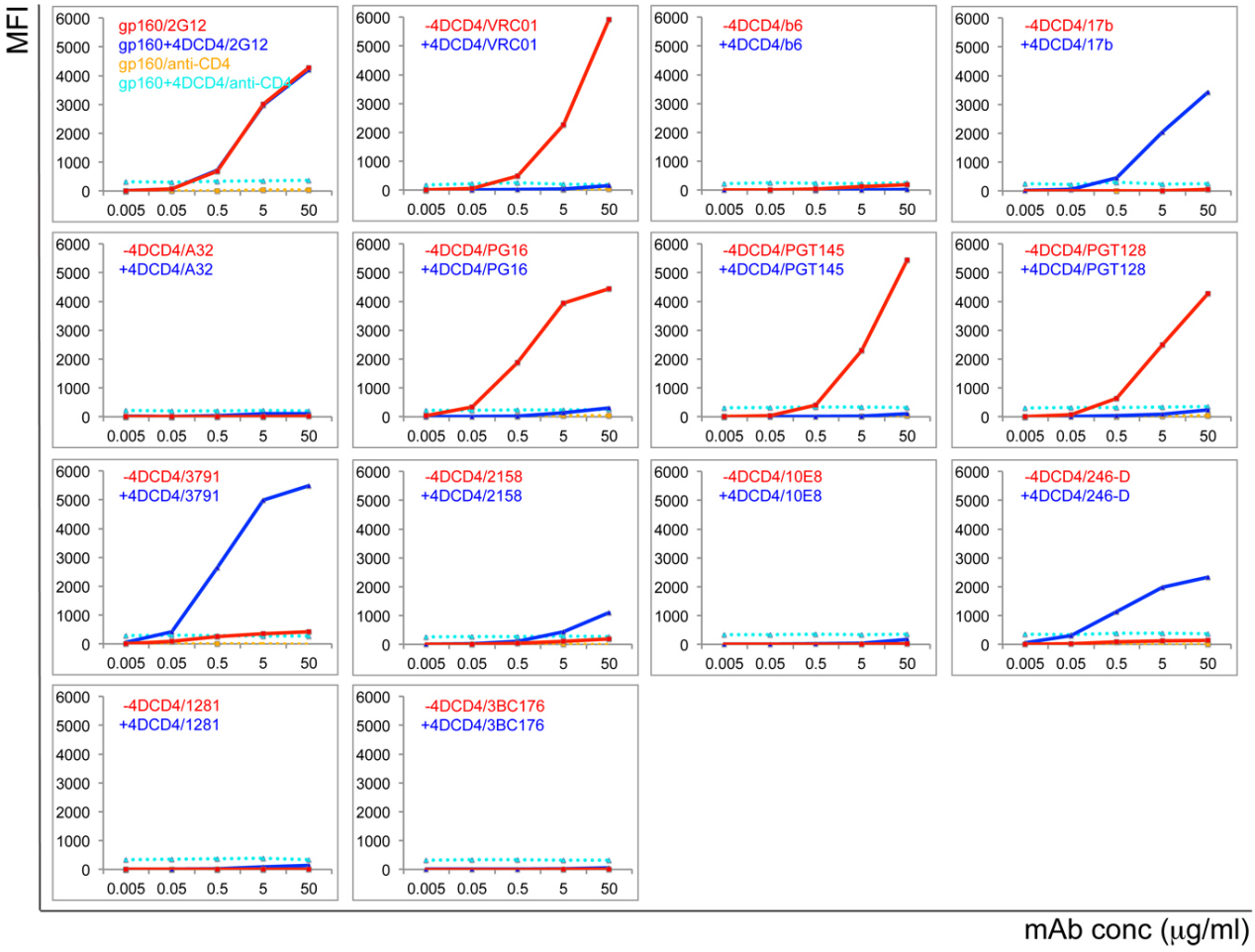
MFI
gp160/2G12
gp160+4DCD4/2G12
gp160/anti-CD4
gp160+4DCD4/anti-CD4
-4DCD4/VRC01
+4DCD4/VRC01
-4DCD4/b6
+4DCD4/b6
-4DCD4/17b
+4DCD4/17b
-4DCD4/A32
+4DCD4/A32
-4DCD4/PG16
+4DCD4/PG16
-4DCD4/PGT145
+4DCD4/PGT145
-4DCD4/PGT128
+4DCD4/PGT128
-4DCD4/3791
+4DCD4/3791
-4DCD4/2158
+4DCD4/2158
-4DCD4/10E8
+4DCD4/10E8
-4DCD4/246-D
+4DCD4/246-D
-4DCD4/1281
+4DCD4/1281
-4DCD4/3BC176
+4DCD4/3BC176
0 1000 2000 3000 4000 5000 6000
0.005 0.05 0.5 5 50
mAb conc (μg/ml)

C (Fig. S5C)

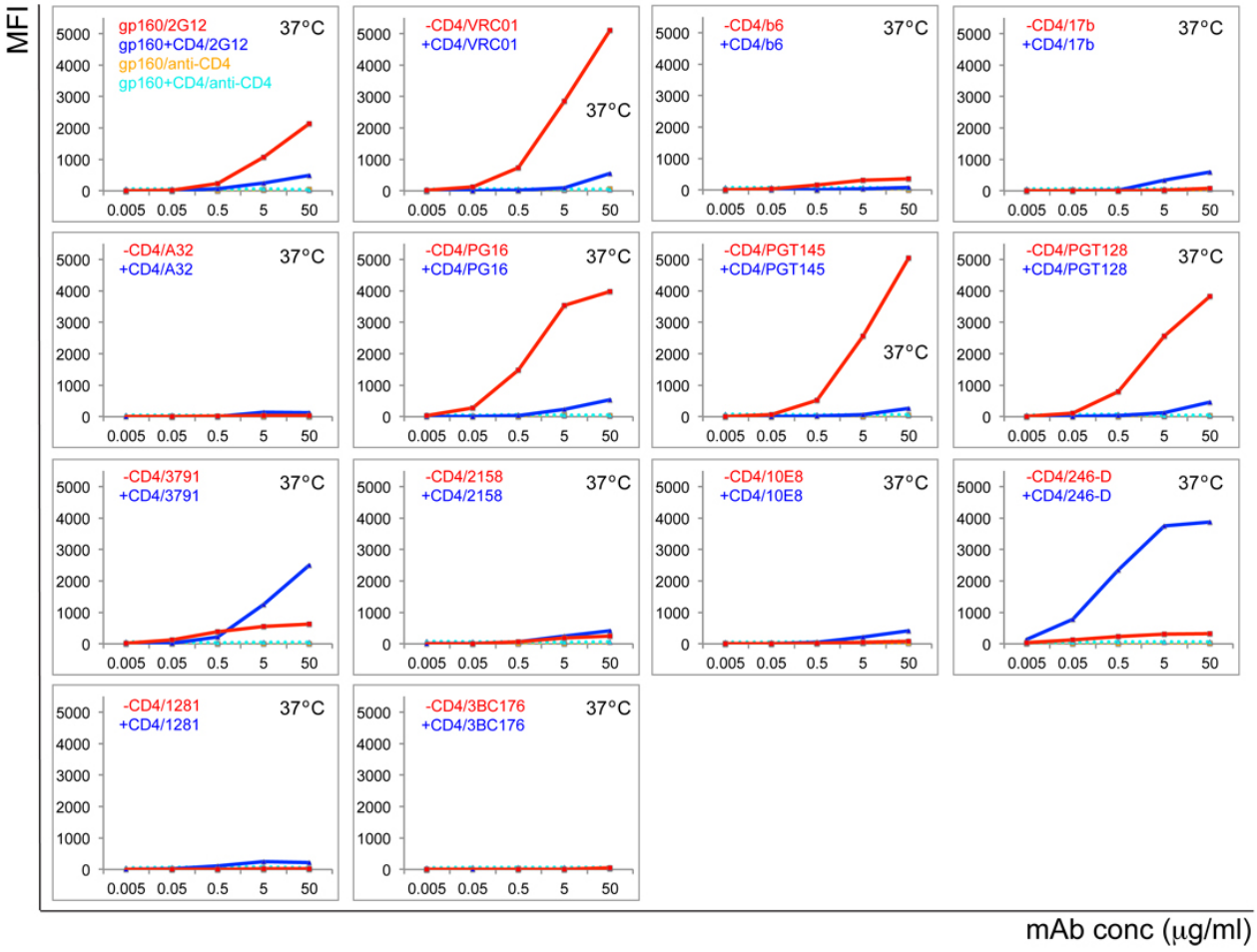

Fig. S5. Additional antigenic characteristics of the 92UG037.8 gp160 presented on cell surfaces. (A) Plots of binding by additional antibodies to the Env trimer on the 92UG037.8 gp160 cell surfaces in the absence (red) or presence (blue) of soluble CD4. Fluorescent signal for bound CD4 is shown in the presence of CD4 (cyan) or in the absence of CD4 (orange). Antibodies and their epitopes are indicated. The IC50 values were determined in a luciferase-based virus neutralization assay using 92UG037.8 gp160 and purified antibodies. Unless specified, all antibodies used are Fab fragments. (**B**) Plots of binding by selected antibodies to the Env trimer on the 92UG037.8 gp160 cell surfaces in the absence (red) or presence (blue) of 4 domain CD4. (**C**) Plots of binding by selected antibodies to the Env trimer on the 92UG037.8 gp160 cell surfaces in the absence (red) or presence (blue) of soluble CD4 at 37°C. Original flow cytometry histograms are shown

in figs. S6-S8. Extensive control experiments were carried out to ensure the binding specificity and the experiments were repeated at least two times with almost identical results.

Fig. S6.

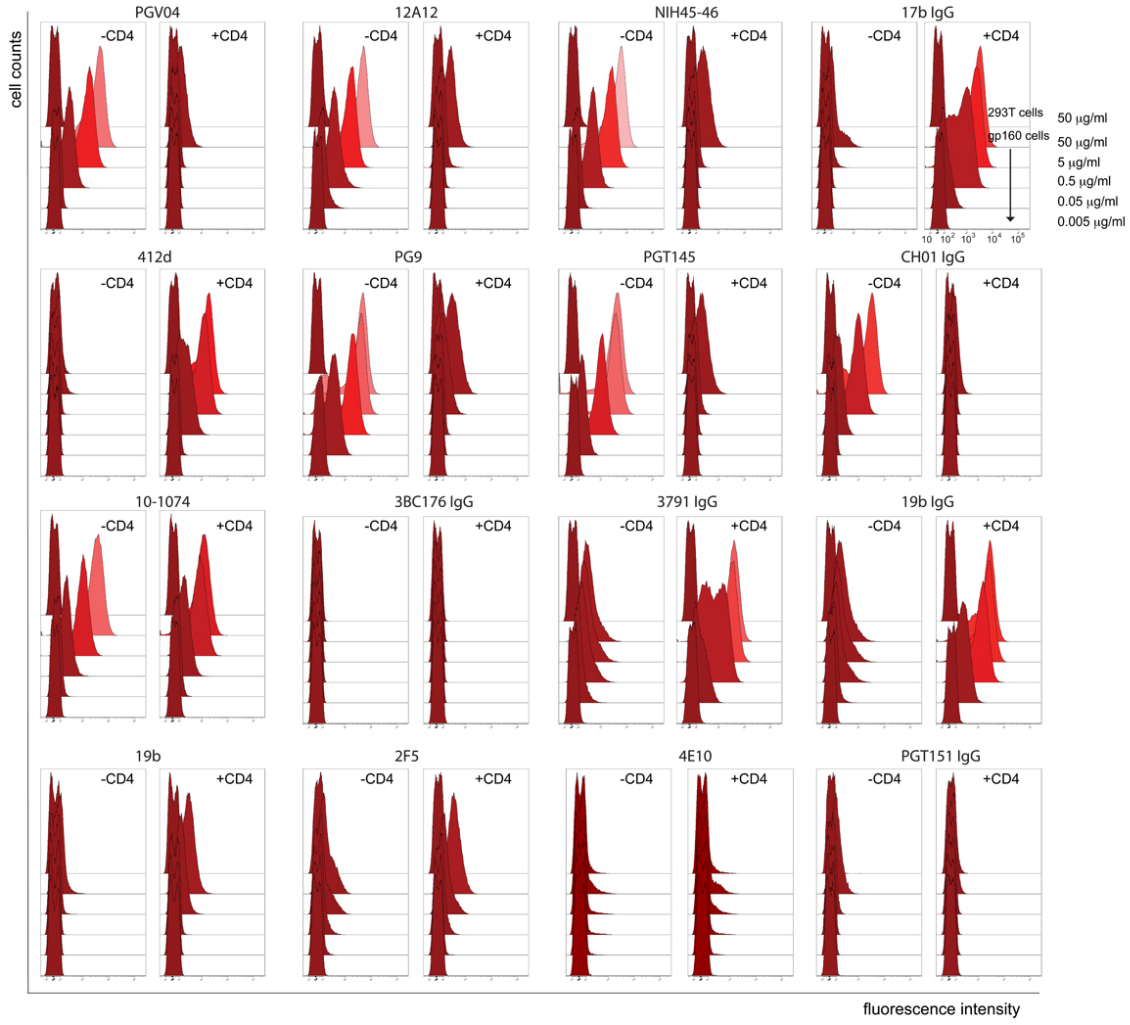
PGV04
12A12
NIH45-46
17b IgG
412d
PG9
PGT145
CH01 IgG
10-1074
3BC176 IgG
3791 IgG
19b IgG
19b
2F5
4E10
PGT151 IgG
-CD4
+CD4
cell counts
fluorescence intensity
293T cells
gp160 cells
50 μg/ml
50 μg/ml
5 μg/ml
0.5 μg/ml
0.05 μg/ml
0.005 μg/ml

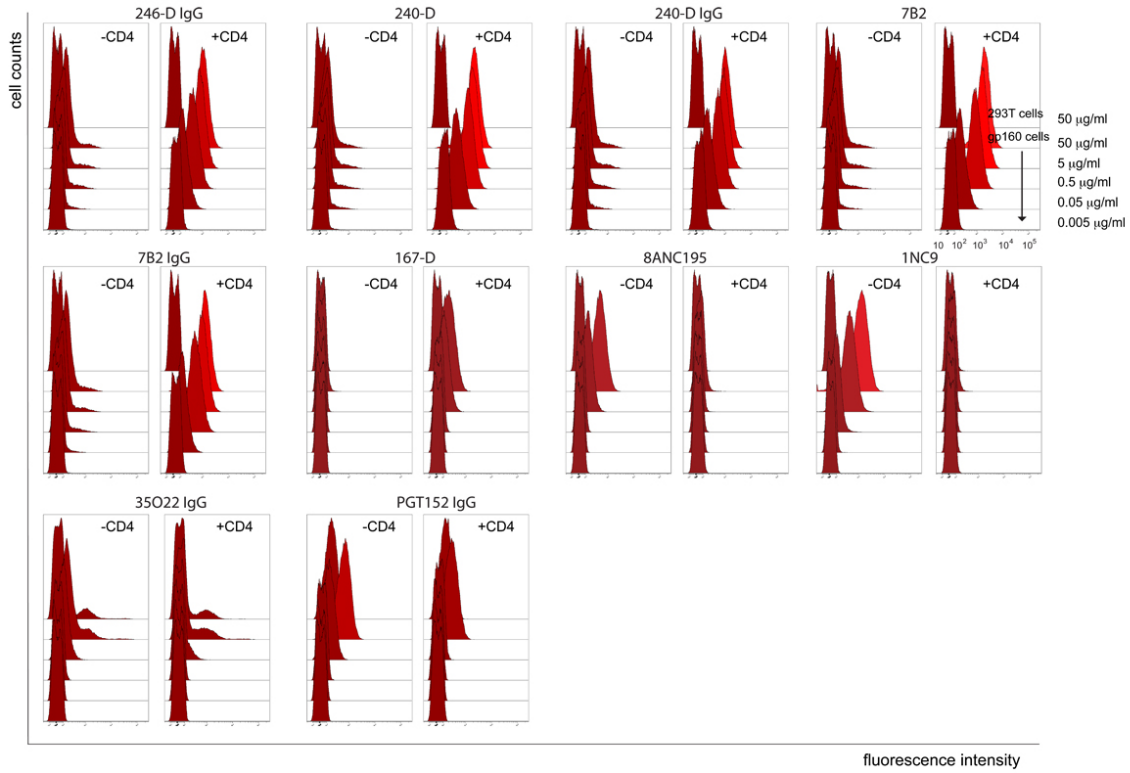

Fig. S6. Flow cytometry histograms of antibody binding to the Env trimer on the 92UG037.8 gp160 cell surfaces by a FACS assay. Data are summarized in fig. S5A.

Fig. S7.

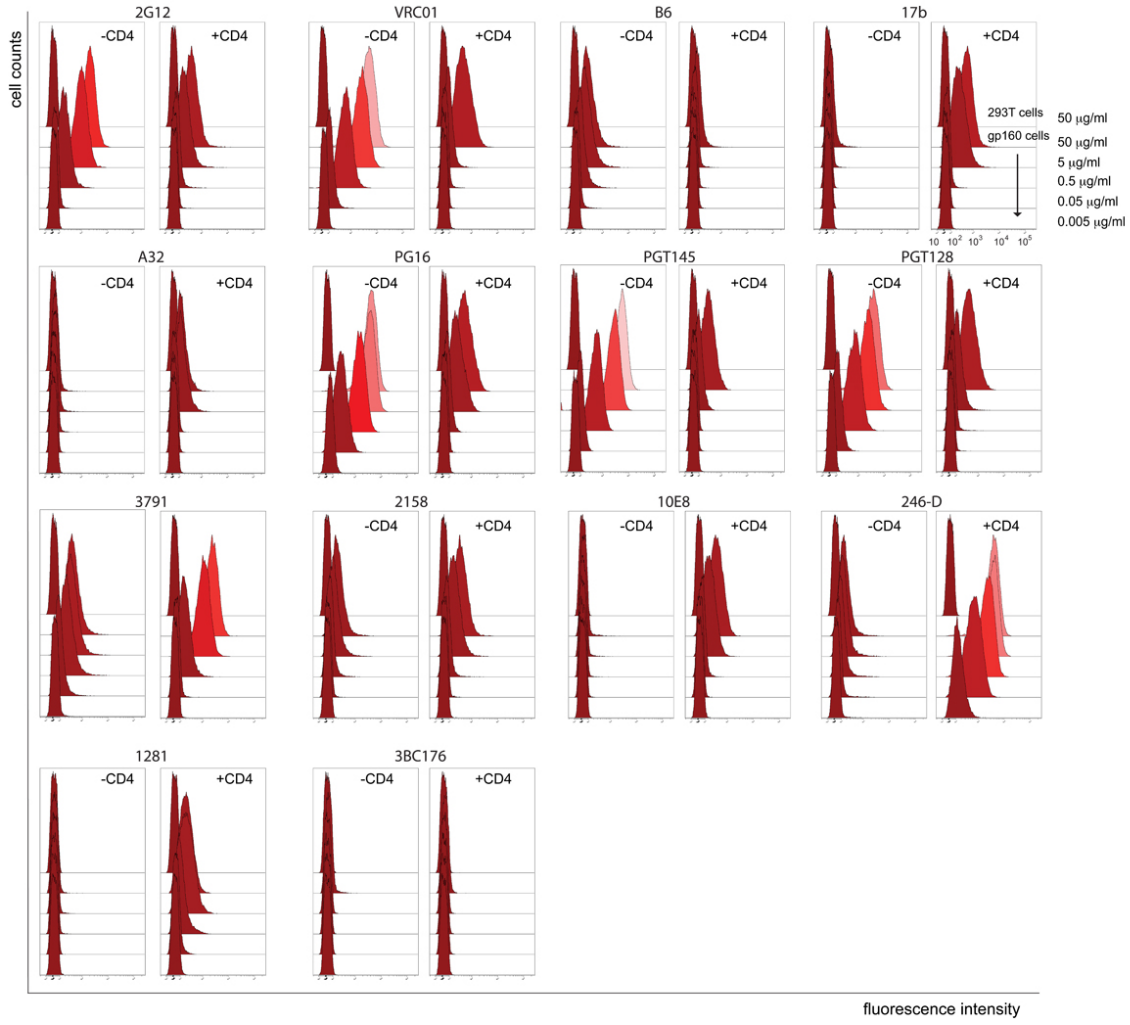

Fig. S7. Flow cytometry histograms of antibody binding to the Env trimer on the 92UG037.8 gp160 cell surfaces by a FACS assay. Data are summarized in fig. S5B.

Fig. S8.

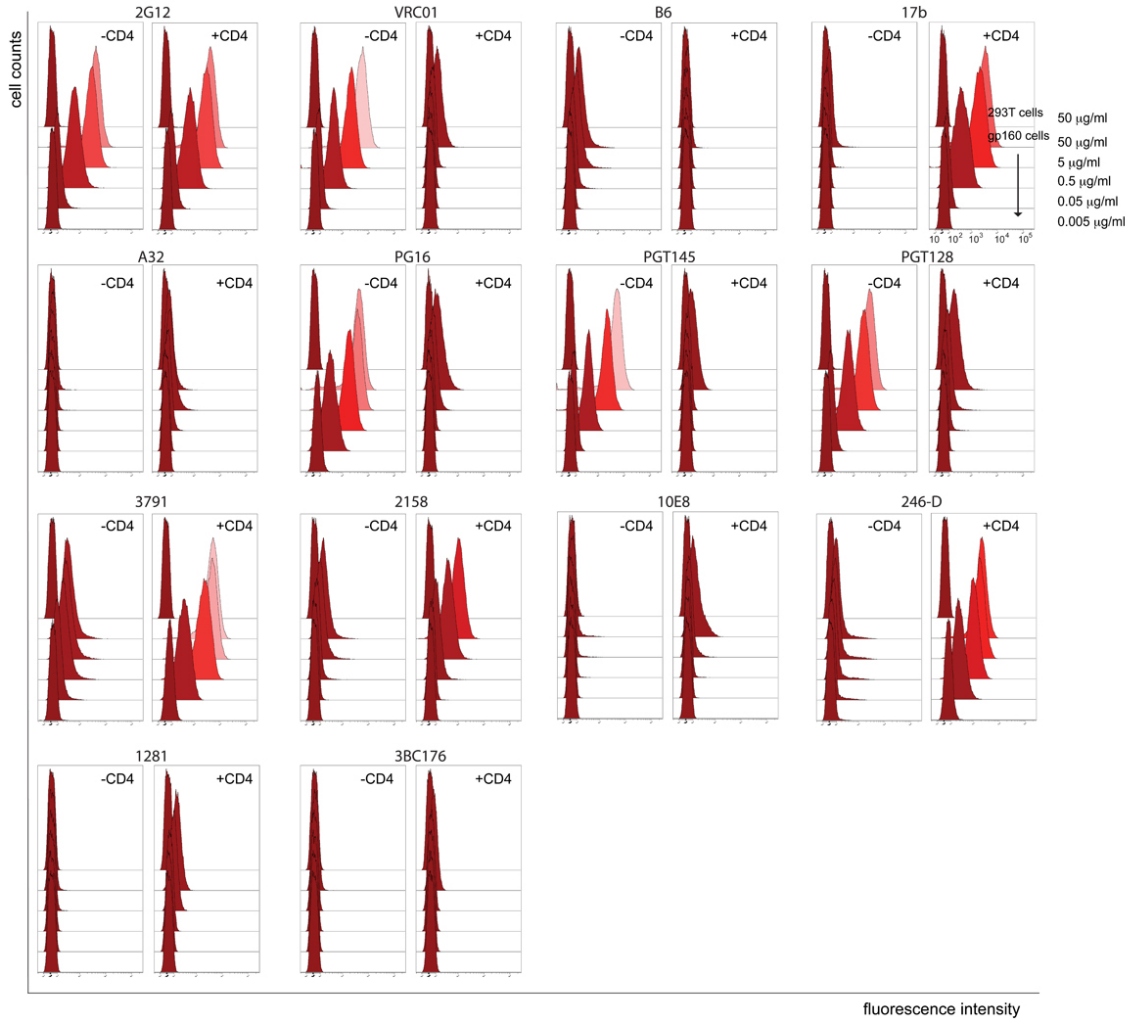

Fig. S8. Flow cytometry histograms of antibody binding to the Env trimer on the 92UG037.8 gp160 cell surfaces by a FACS assay. Data are summarized in fig. S5C.

Fig. S9.

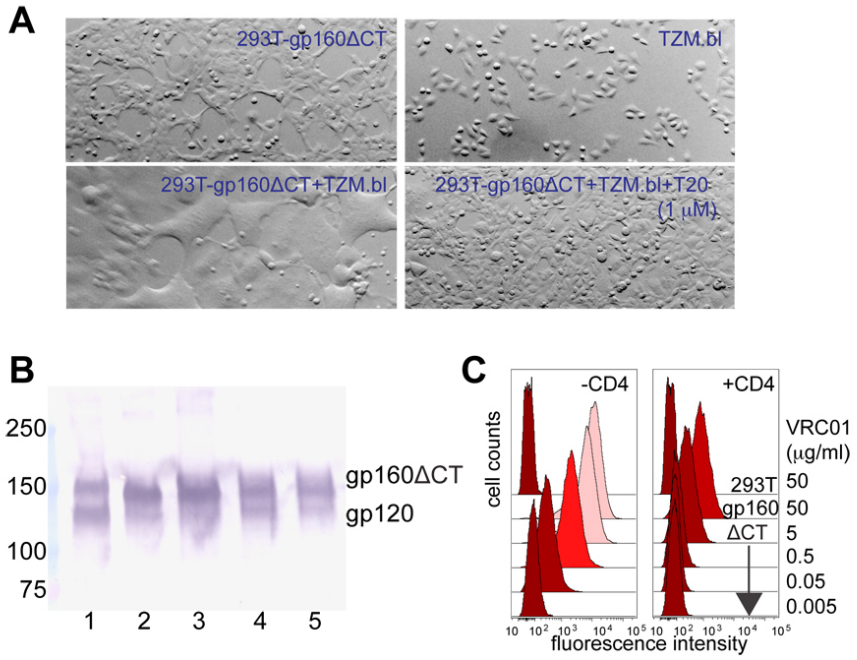

Fig. S9. Characterization of the 92UG037.8 gp160-ΔCT. (**A**) 92UG037.8 gp160-ΔCT mediated cell-cell fusion. 293T cells stably transfected with 92UG037.8 gp160-ΔCT (293T- gp160-ΔCT) were mixed with TZM-bl cells in the absence or presence of the fusion inhibitor T20. (**B**) Env samples prepared from the 92UG037.8 gp160-ΔCT stable cell line are detected by a V3 antibody 3791. Lane1, total cell lysate of 92UG037.8 gp160 at a control; lane 2, total cell lysate of 92UG037.8 gp160-ΔCT stable cell line; lane 3, membrane fraction of the gp160-ΔCT cell; lane 4 and 5, Env trimers on the 92UG037.8 gp160-ΔCT cell surfaces immunoprecipitated by antibody VRC01 and PGT128, respectively. (**C**) Flow cytometry histograms of VRC01 binding to the Env trimer on the 92UG037.8 gp160-ΔCT cell surfaces in the absence or presence of soluble CD4. VRC01 concentration varies from 0.005 to 50 μg/ml. VRC01 binding at 50 μg/ml to 293T cells is a negative control.

Fig. S10.

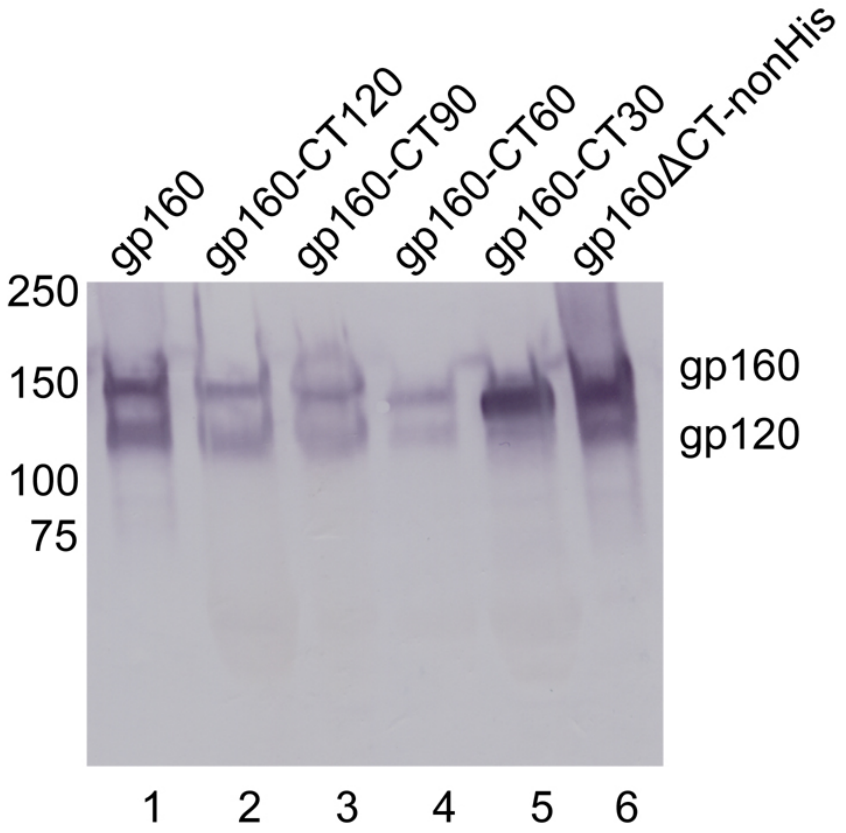

Fig. S10. Western blot of Env samples of various gp160 constructs. Env samples prepared from the stable cell lines expressing gp160 (lane 1), gp160-CT120 (lane 2), gp160-CT90 (lane 3), gp160-CT60 (lane 4), gp160-CT30 (lane 5) and gp160ΔCT-nonHis (lane 6) are detected by a V3 antibody 3791.

Fig. S11.

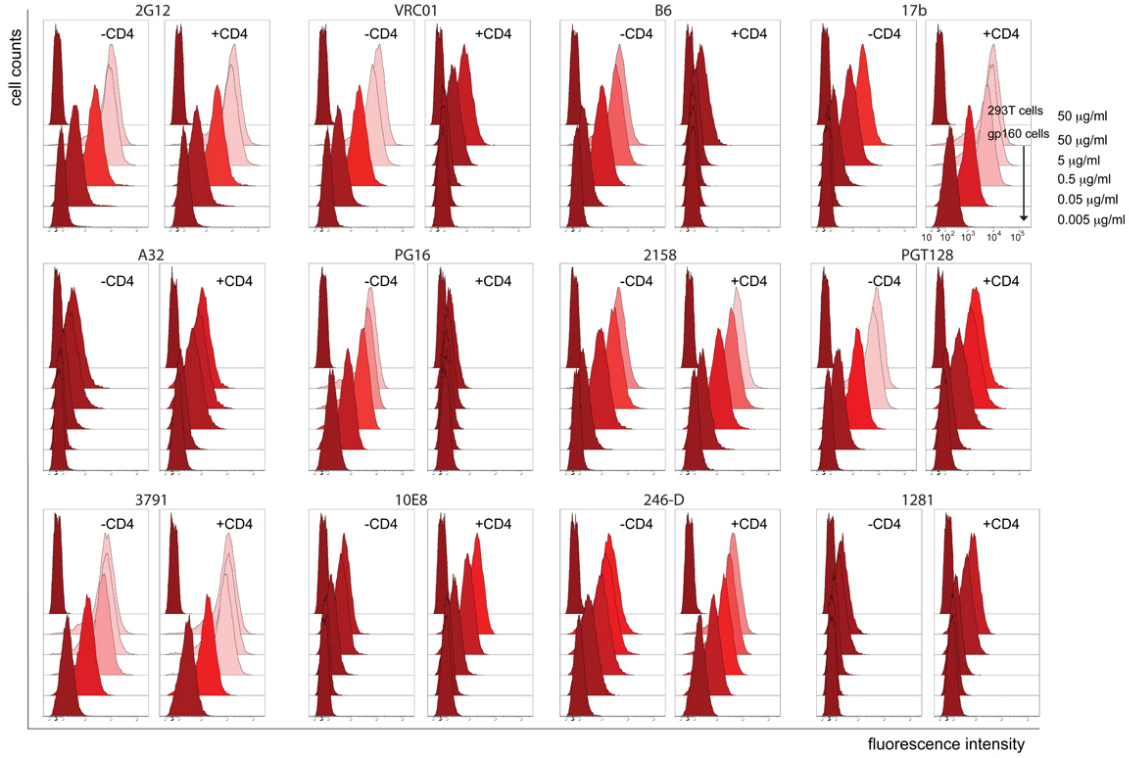

Fig. S11. Flow cytometry histograms of antibody binding to the Env trimer on the 92UG037.8 gp160ΔCT cell surfaces by a FACS assay. Data are summarized in fig. 2.

Fig. S12.

A (Fig. S12A)

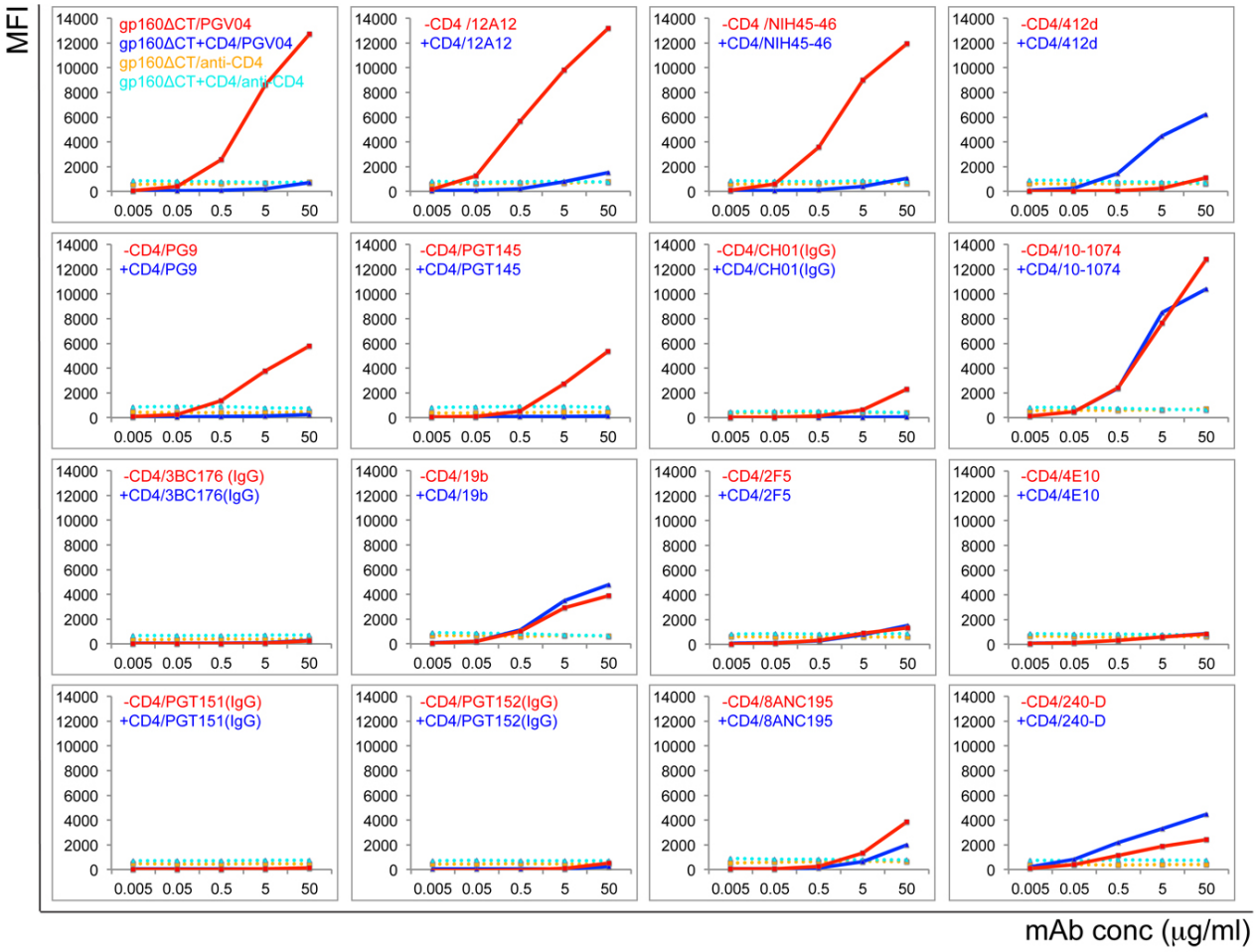

A (Fig. S12A) continued

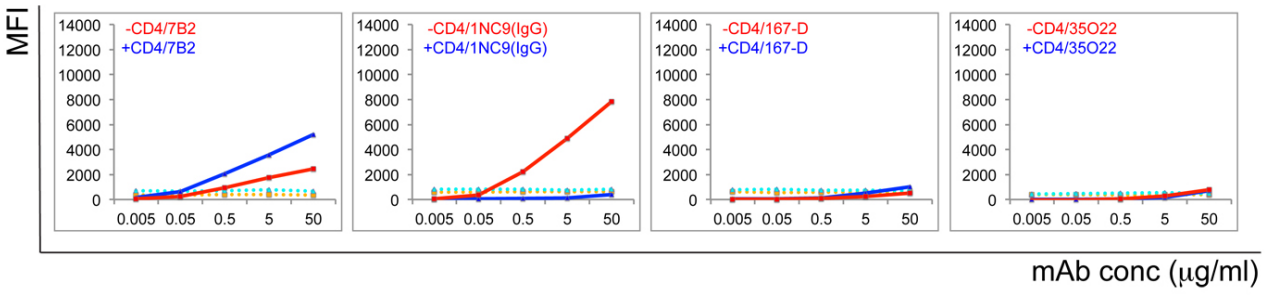

B (Fig. S12B)

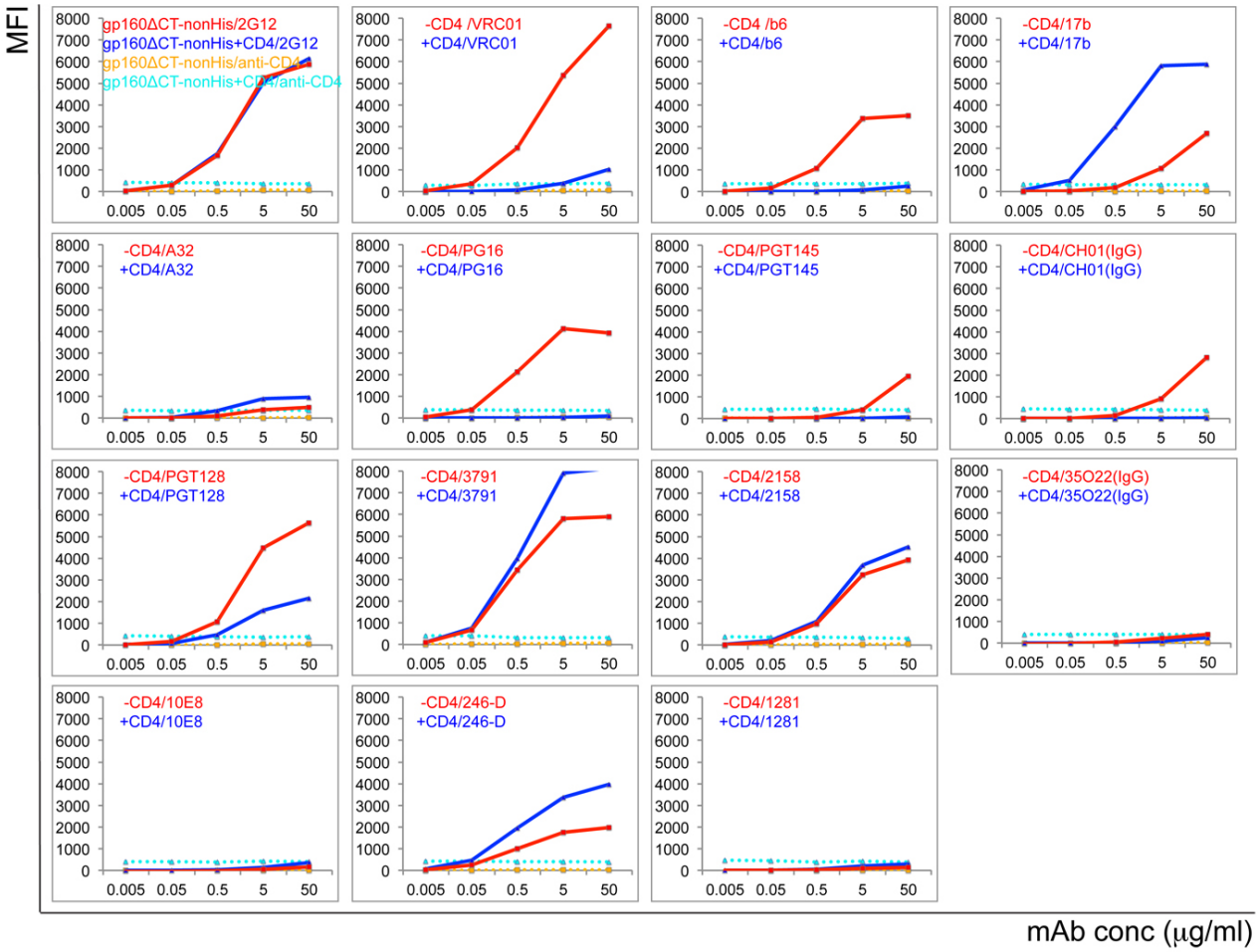

Fig. S12. Additional antigenic properties of the 92UG037.8 gp160-ΔCT presented on cell surfaces. **(A)** Plots of binding by additional antibodies to the Env trimer on the 92UG037.8 gp160-ΔCT cell surfaces in the absence (red) or presence (blue) of soluble CD4. Unless specified, all antibodies used are Fab fragments. Fluorescent signal for bound CD4 is shown in the presence of CD4 (cyan) or in the absence of CD4 (orange). (**B**) Plots of binding by selected antibodies to the Env trimer on the 92UG037.8 gp160ΔCT-nonhis cell surfaces in the absence (red) or presence (blue) of soluble CD4. The 92UG037.8 gp160ΔCT-nonHis does not contain a histag at its C-terminus. Original flow cytometry histograms are shown in figs. S13 and S15. The experiments were repeated at least two times with almost identical results.

Fig. S13.

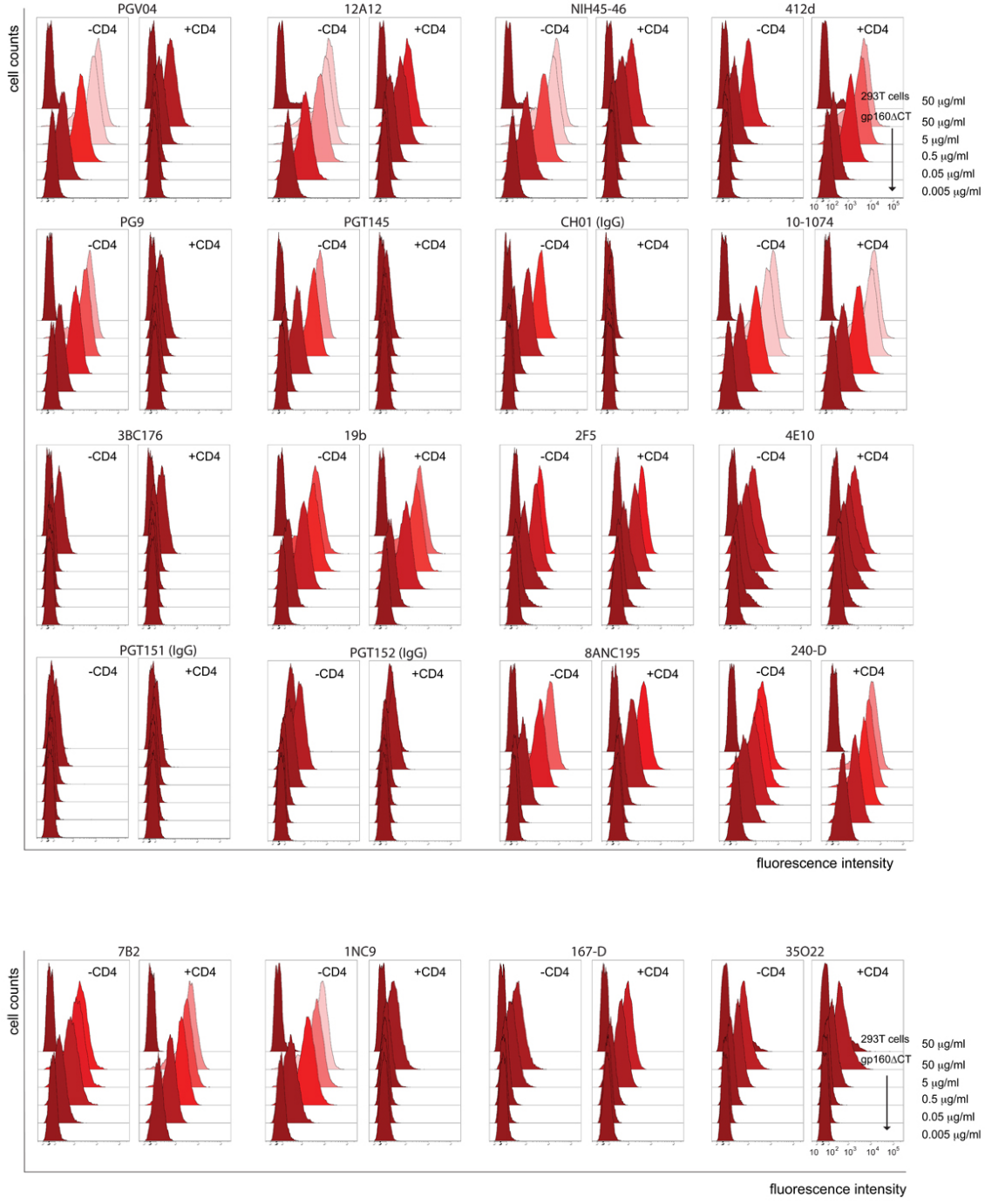

.

Fig. S13. Flow cytometry histograms of antibody binding to the Env trimer on the 92UG037.8 gp160ΔCT cell surfaces by a FACS assay. Data are summarized in fig. S12A.

Fig. S14.

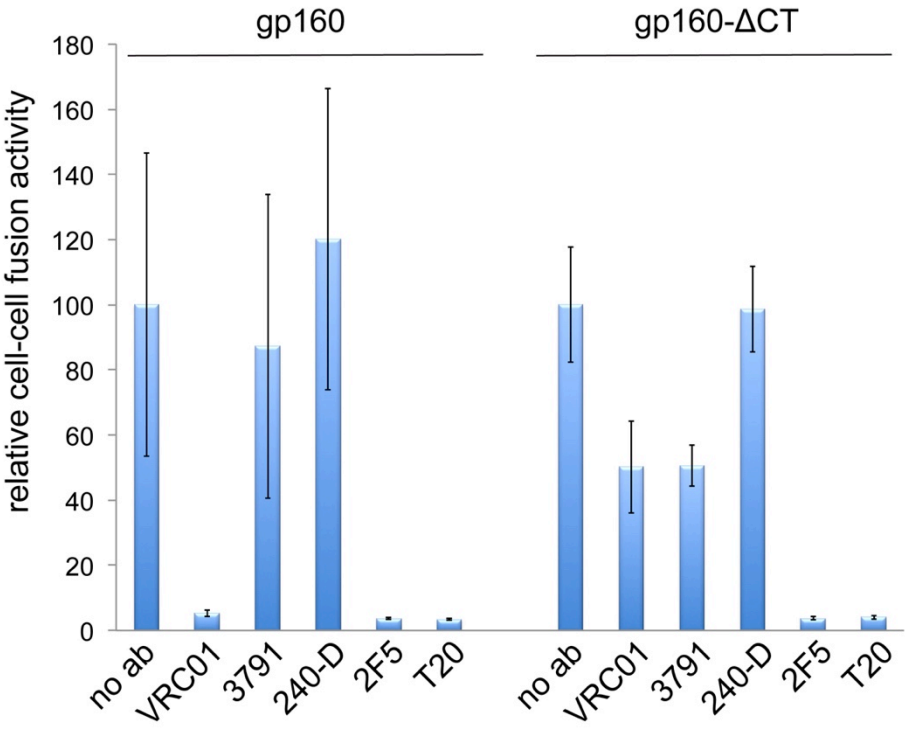

Fig. S14. Inhibition of cell-cell fusion mediated by 92UG037.8 gp160 and 92UG037.8 gp160-ΔCT. 293T cells, transiently cotransfected with the 92UG037.8 gp160 or 92UG037.8 gp160-ΔCT expression construct and a plasmid expressing T7 polymerase, were mixed with CD4-and CCR5-expressing cells with a luciferase reporter gene under the control of a T7 promotor. Cell-cell fusion led to expression of luciferase and thus fusion activity was measured by a luciferase assay. Inhibition of cell-cell fusion was indicated by decrease of fusion activity when a monoclonal antibody or the fusion inhibitor T20 is present. The experiment was carried out in triplicate and repeated at least three times with similar results. Error bars indicate the standard deviation calculated by the Excel STDEV function.

Fig. S15.

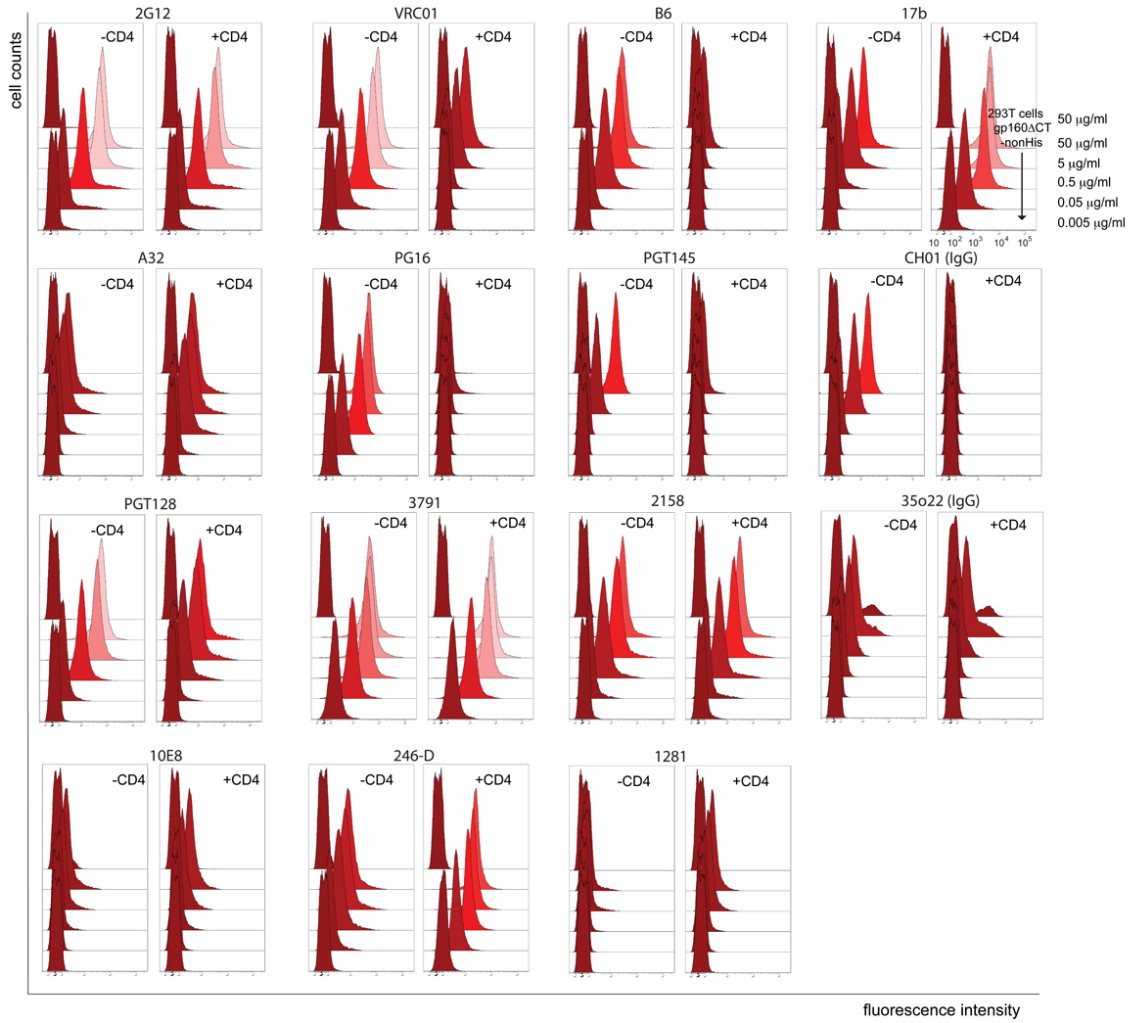

Fig. S15. Flow cytometry histograms of antibody binding to the Env trimer on the 92UG037.8 gp160ΔCT-nonHis cell surfaces by a FACS assay. Data are summarized in fig. S12B.

Fig. S16.

A (Fig. S16A)

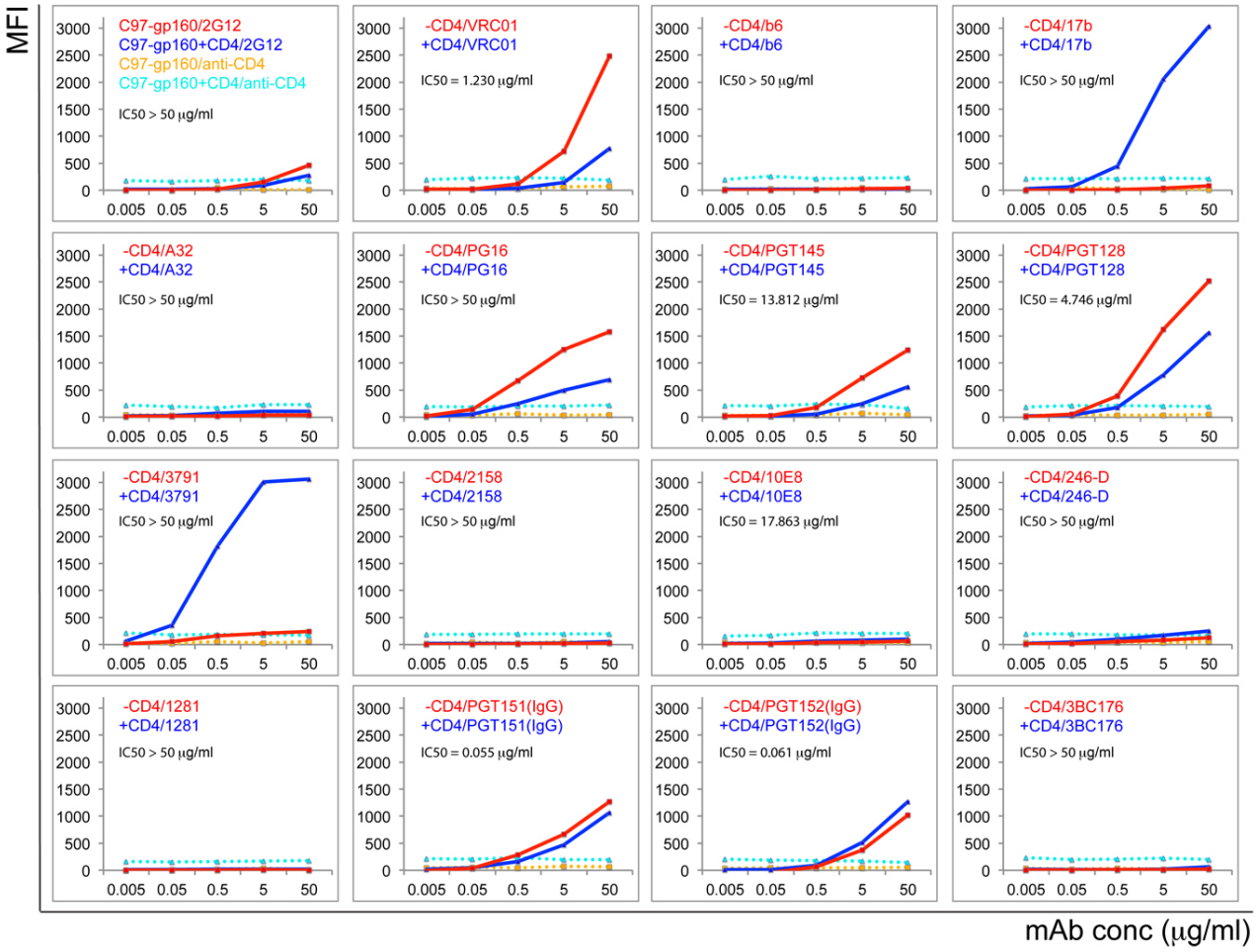

B (Fig. S16B)

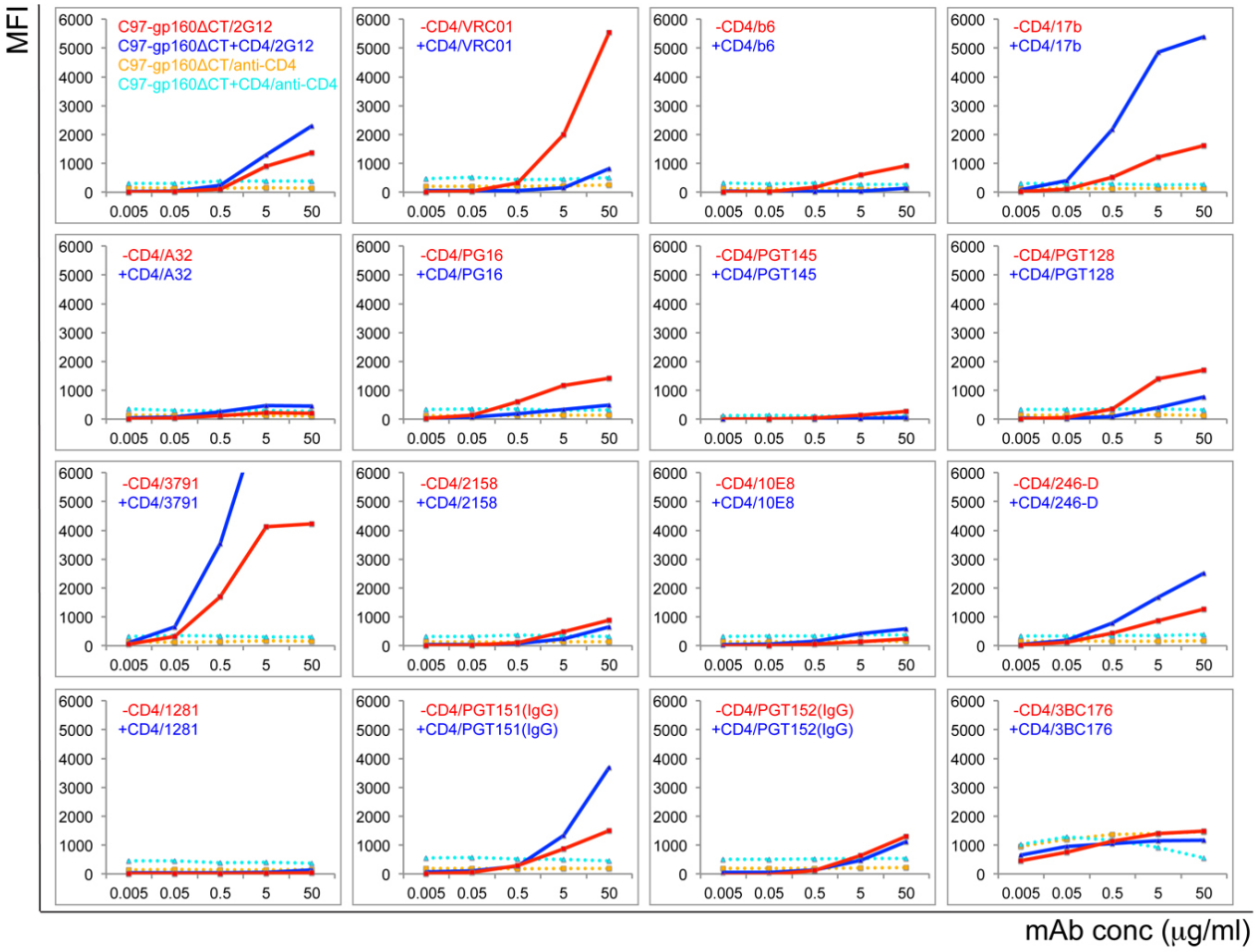

Fig. S16. Antigenic properties of the C97ZA012 gp160 and C97ZA012gp160ΔCT presented on cell surfaces. (**A**) Plots of binding by selected antibodies to the Env trimer on the C97ZA012 gp160 cell surfaces in the absence (red) or presence (blue) of soluble CD4. Fluorescent signal for bound CD4 is shown in the presence of CD4 (cyan) or in the absence of CD4 (orange). Unless specified, all antibodies used are Fab fragments. (**B**) Plots of binding by selected antibodies to the Env trimer on the C97ZA012gp160ΔCT cell surfaces in the absence (red) or presence (blue) of CD4. Original flow cytometry histograms are shown in figs. S17 and S18. The experiments were repeated at least two times with almost identical results.

Fig. S17.

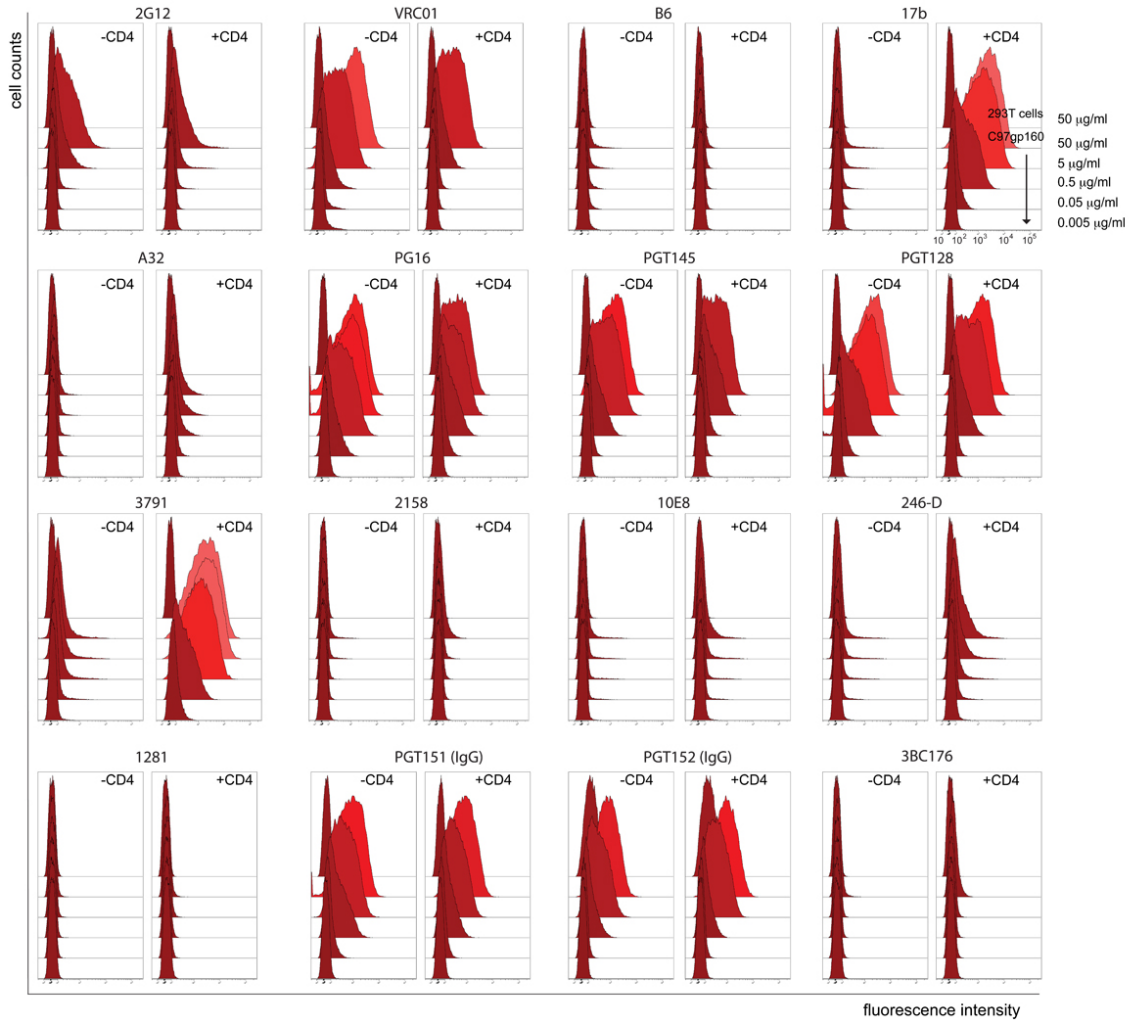

Fig. S17. Flow cytometry histograms of antibody binding to the Env trimer on the C97ZA012 gp160 cell surfaces by a FACS assay. Data are summarized in fig. S16A.

Fig. S18.

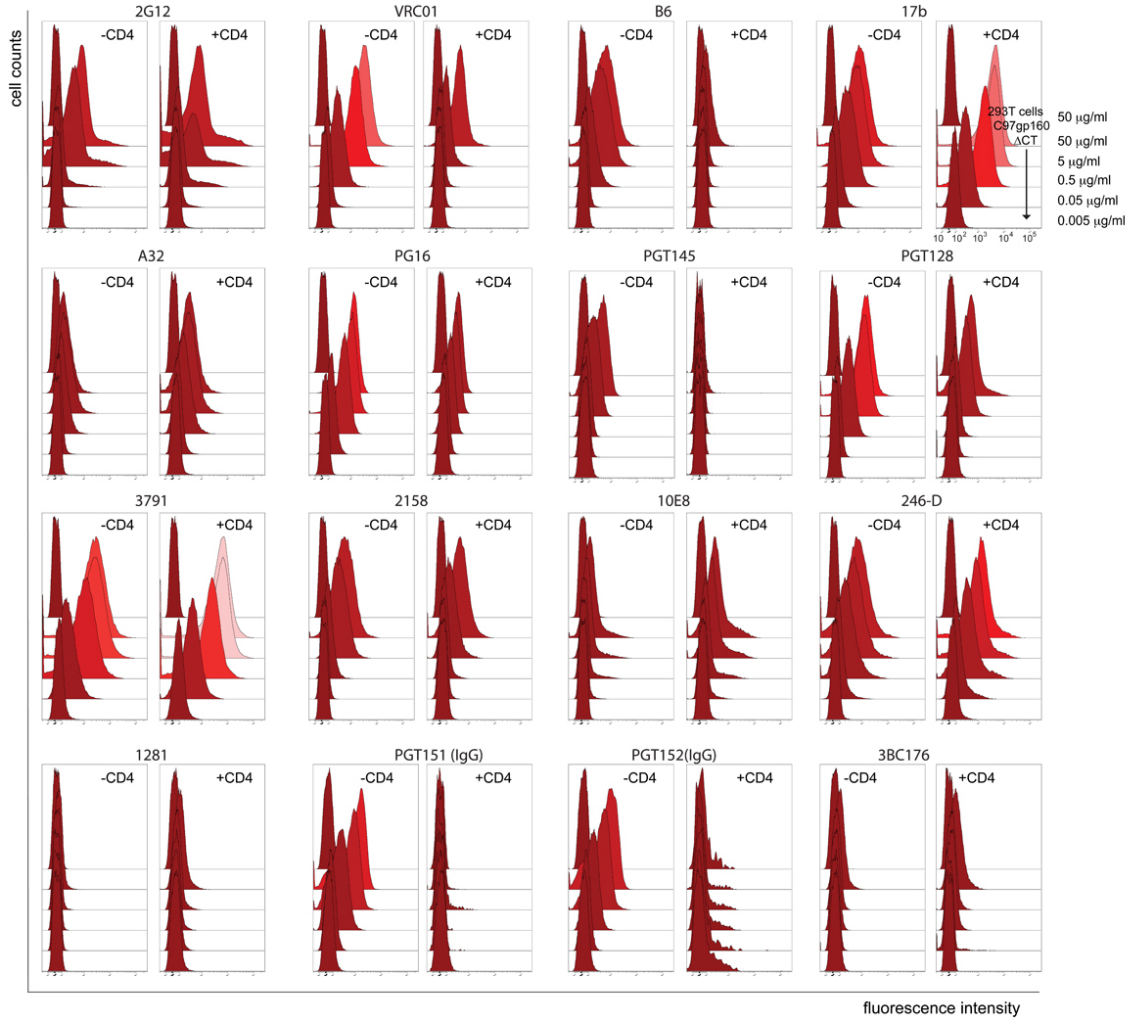

Fig. S18. Flow cytometry histograms of antibody binding to the Env trimer on the C97ZA012 gp160ΔCT cell surfaces by a FACS assay. Data are summarized in fig. S16B.

Fig. S19.

A (Fig. S19A)

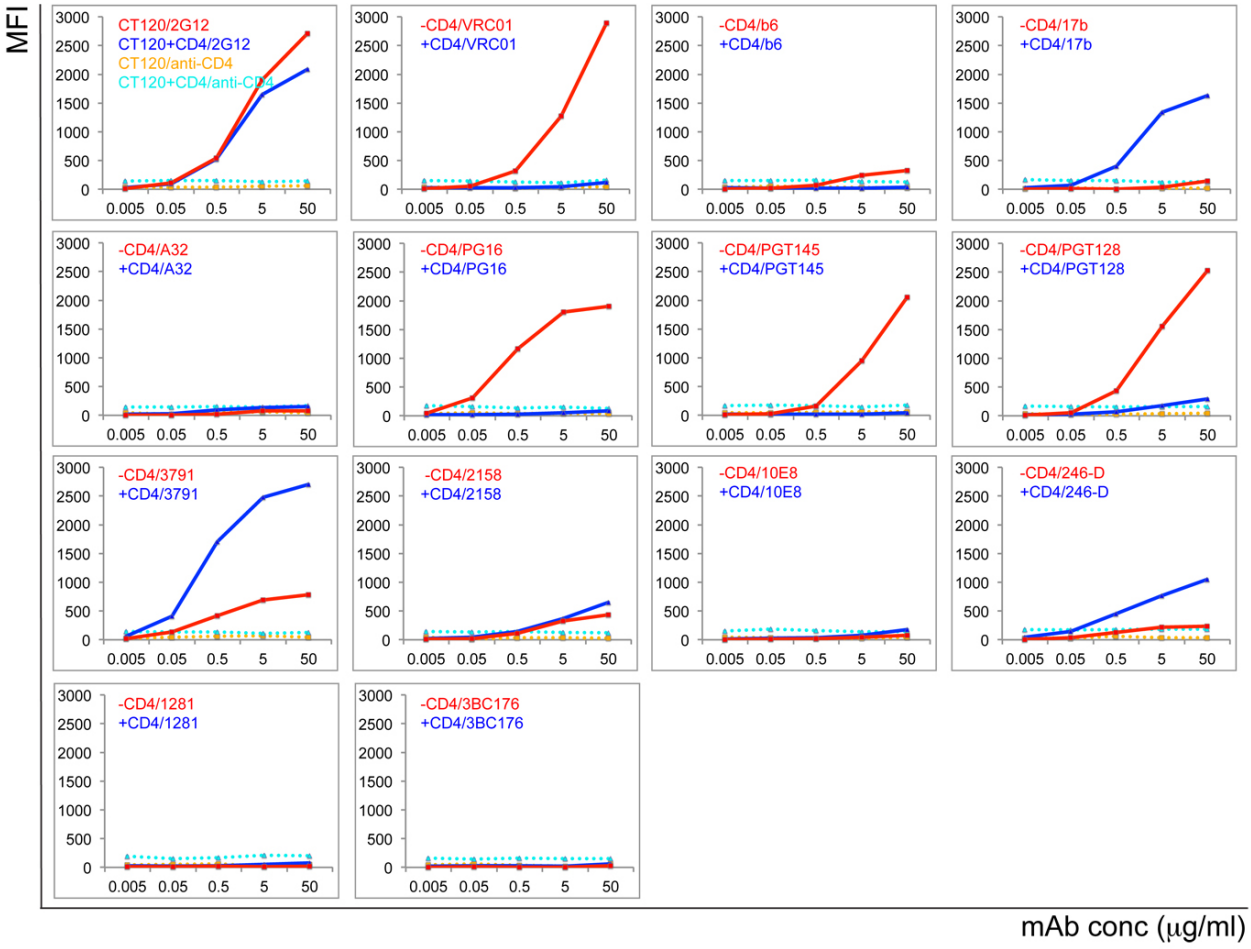

B (Fig. S19B)

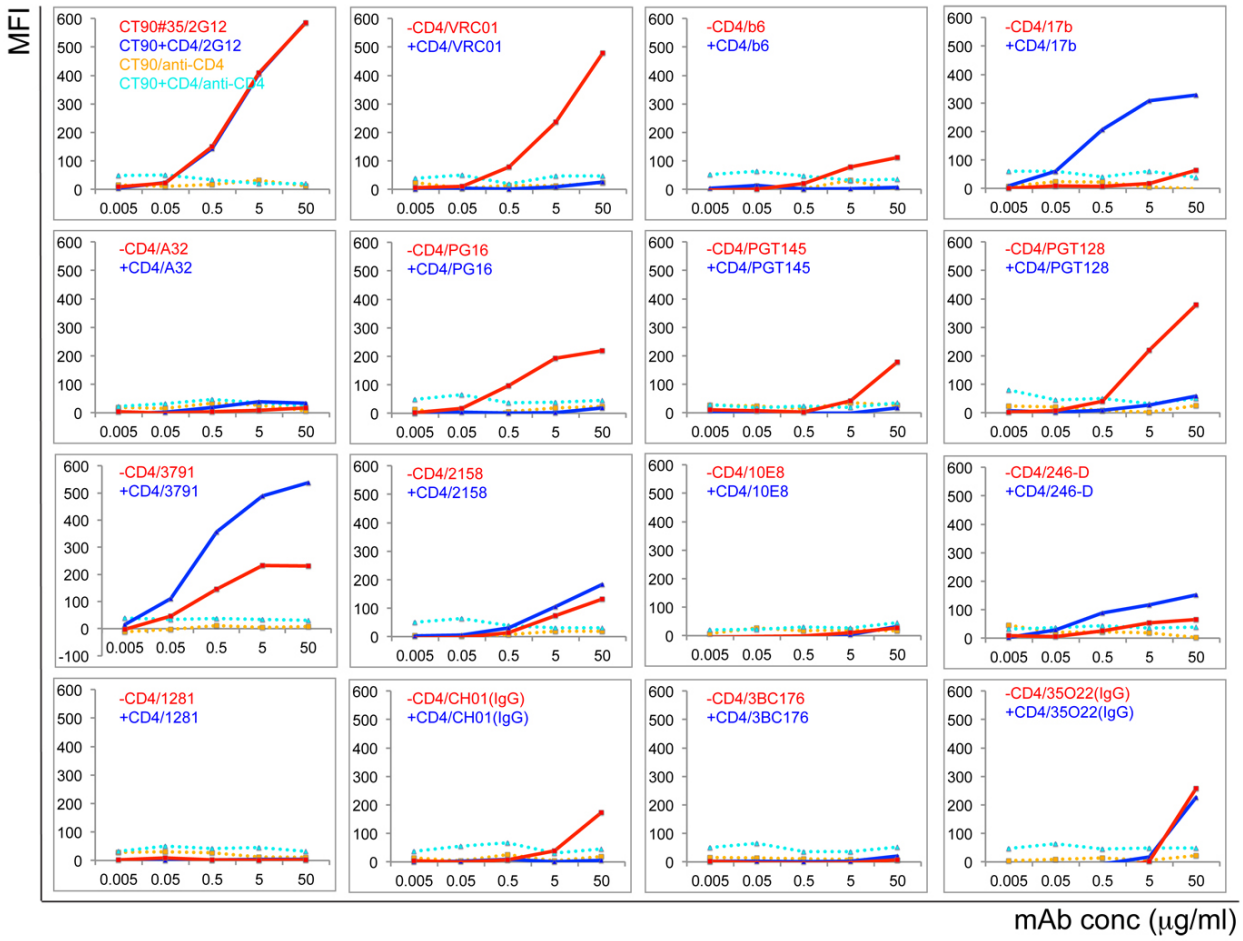
MFI
CT90#35/2G12
CT90+CD4/2G12
CT90/anti-CD4
CT90+CD4/anti-CD4
-CD4/VRC01
+CD4/VRC01
-CD4/b6
+CD4/b6
-CD4/17b
+CD4/17b
-CD4/A32
+CD4/A32
-CD4/PG16
+CD4/PG16
-CD4/PGT145
+CD4/PGT145
-CD4/PGT128
+CD4/PGT128
-CD4/3791
+CD4/3791
-CD4/2158
+CD4/2158
-CD4/10E8
+CD4/10E8
-CD4/246-D
+CD4/246-D
-CD4/1281
+CD4/1281
-CD4/CH01(IgG)
+CD4/CH01(IgG)
-CD4/3BC176
+CD4/3BC176
-CD4/35O22(IgG)
+CD4/35O22(IgG)
0.005 0.05 0.5 5 50
mAb conc (μg/ml)

C (Fig. S19C)

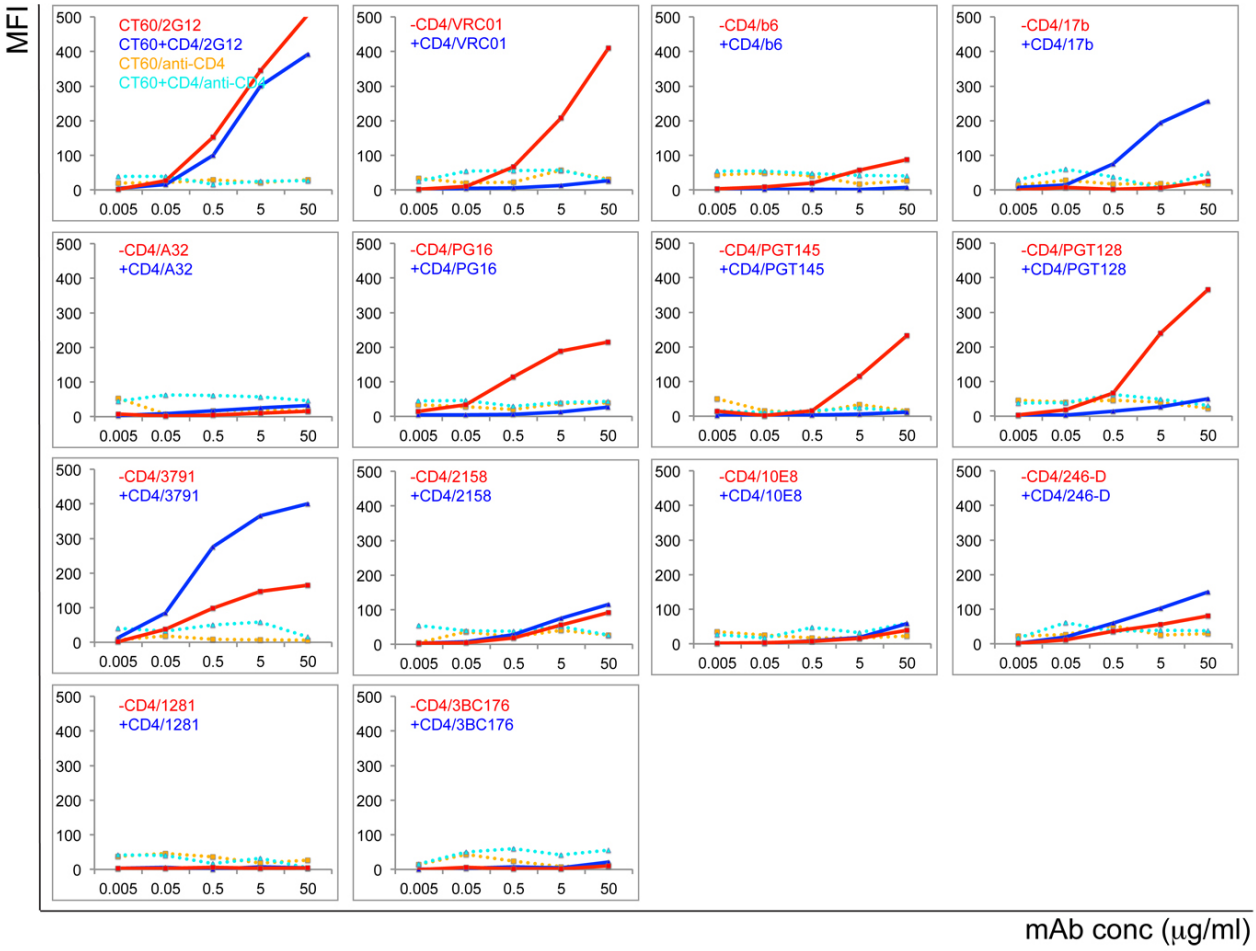
MFI
CT60/2G12
CT60+CD4/2G12
CT60/anti-CD4
CT60+CD4/anti-CD4
-CD4/VRC01
+CD4/VRC01
-CD4/b6
+CD4/b6
-CD4/17b
+CD4/17b
-CD4/A32
+CD4/A32
-CD4/PG16
+CD4/PG16
-CD4/PGT145
+CD4/PGT145
-CD4/PGT128
+CD4/PGT128
-CD4/3791
+CD4/3791
-CD4/2158
+CD4/2158
-CD4/10E8
+CD4/10E8
-CD4/246-D
+CD4/246-D
-CD4/1281
+CD4/1281
-CD4/3BC176
+CD4/3BC176
0
100
200
300
400
500
0.005 0.05 0.5 5 50
mAb conc (μg/ml)

D (Fig. S19D)

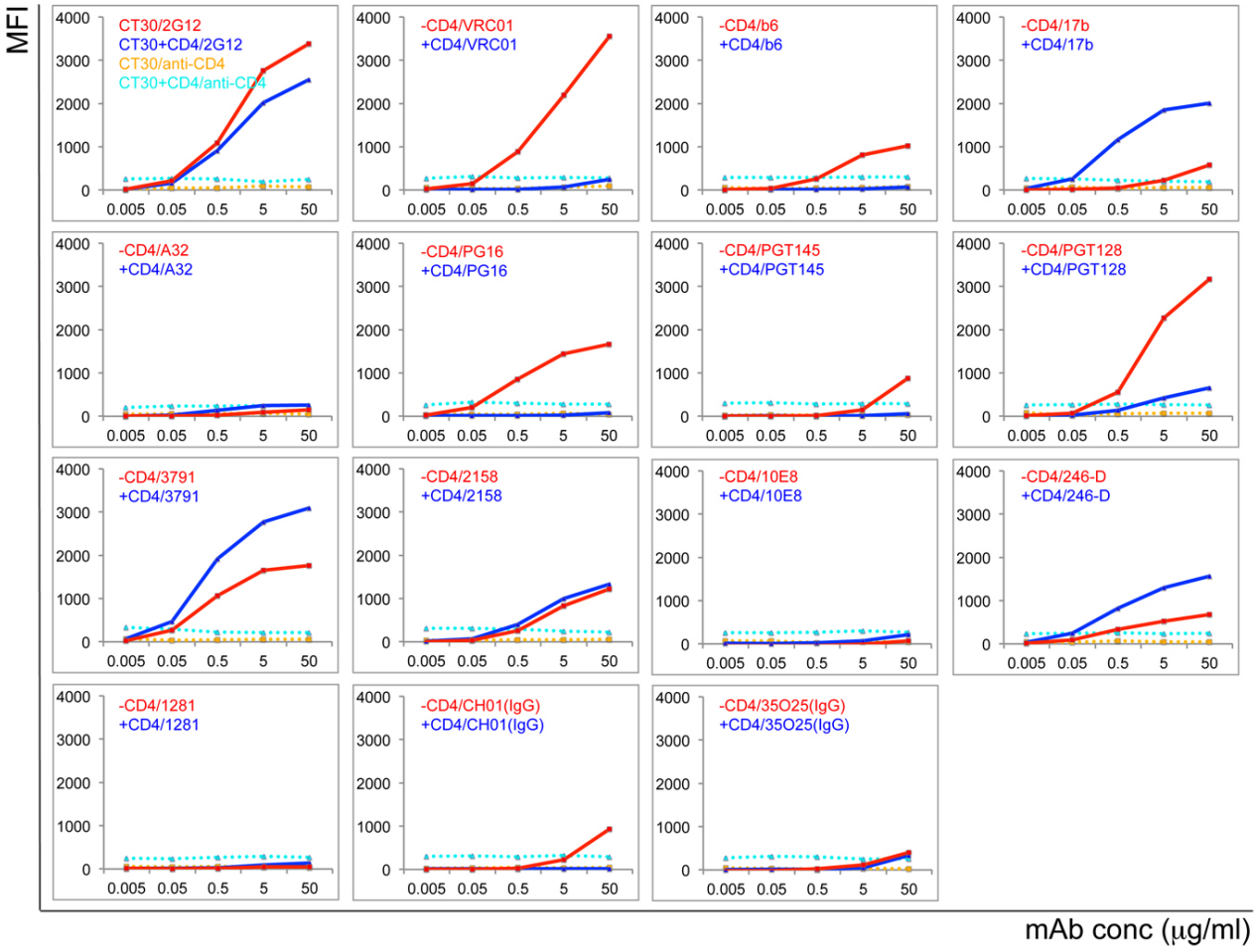
MFI
CT30/2G12
CT30+CD4/2G12
CT30/anti-CD4
CT30+CD4/anti-CD4
-CD4/VRC01
+CD4/VRC01
-CD4/b6
+CD4/b6
-CD4/17b
+CD4/17b
-CD4/A32
+CD4/A32
-CD4/PG16
+CD4/PG16
-CD4/PGT145
+CD4/PGT145
-CD4/PGT128
+CD4/PGT128
-CD4/3791
+CD4/3791
-CD4/2158
+CD4/2158
-CD4/10E8
+CD4/10E8
-CD4/246-D
+CD4/246-D
-CD4/1281
+CD4/1281
-CD4/CH01(IgG)
+CD4/CH01(IgG)
-CD4/35O25(IgG)
+CD4/35O25(IgG)
0 1000 2000 3000 4000
0.005 0.05 0.5 5 50
mAb conc (μg/ml)

E (Fig. S19E)

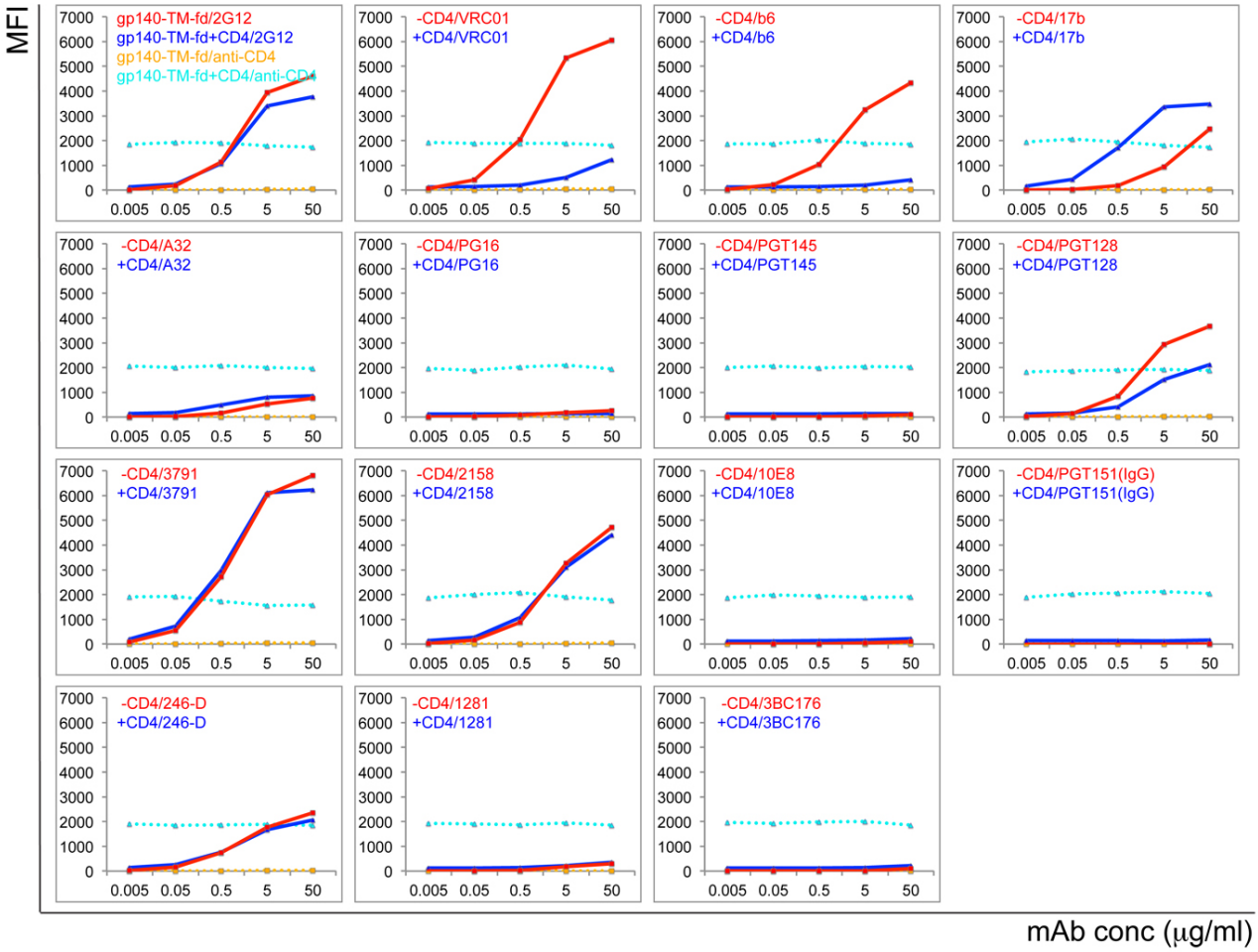
MFI
gp140-TM-fd/2G12
gp140-TM-fd+CD4/2G12
gp140-TM-fd/anti-CD4
gp140-TM-fd+CD4/anti-CD4
-CD4/VRC01
+CD4/VRC01
-CD4/b6
+CD4/b6
-CD4/17b
+CD4/17b
-CD4/A32
+CD4/A32
-CD4/PG16
+CD4/PG16
-CD4/PGT145
+CD4/PGT145
-CD4/PGT128
+CD4/PGT128
-CD4/3791
+CD4/3791
-CD4/2158
+CD4/2158
-CD4/10E8
+CD4/10E8
-CD4/PGT151(IgG)
+CD4/PGT151(IgG)
-CD4/246-D
+CD4/246-D
-CD4/1281
+CD4/1281
-CD4/3BC176
+CD4/3BC176
0 1000 2000 3000 4000 5000 6000 7000
0.005 0.05 0.5 5 50
mAb conc (μg/ml)

F (Fig. S19F)

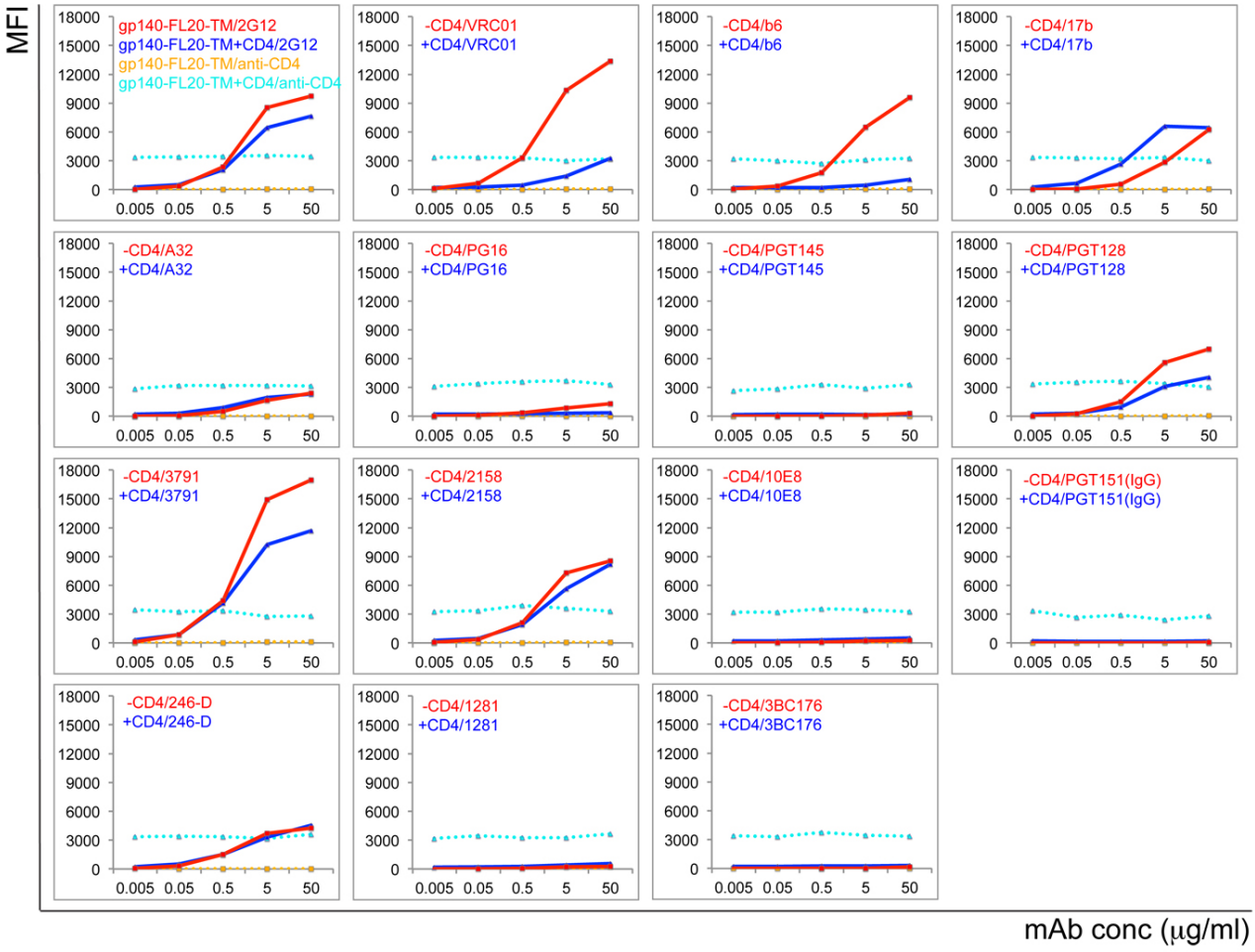
MFI
gp140-FL20-TM/2G12
gp140-FL20-TM+CD4/2G12
gp140-FL20-TM/anti-CD4
gp140-FL20-TM+CD4/anti-CD4
-CD4/VRC01
+CD4/VRC01
-CD4/b6
+CD4/b6
-CD4/17b
+CD4/17b
-CD4/A32
+CD4/A32
-CD4/PG16
+CD4/PG16
-CD4/PGT145
+CD4/PGT145
-CD4/PGT128
+CD4/PGT128
-CD4/3791
+CD4/3791
-CD4/2158
+CD4/2158
-CD4/10E8
+CD4/10E8
-CD4/PGT151(IgG)
+CD4/PGT151(IgG)
-CD4/246-D
+CD4/246-D
-CD4/1281
+CD4/1281
-CD4/3BC176
+CD4/3BC176
18000
15000
12000
9000
6000
3000
0
0.005 0.05 0.5 5 50
mAb conc (μg/ml)

G (Fig. S19G)

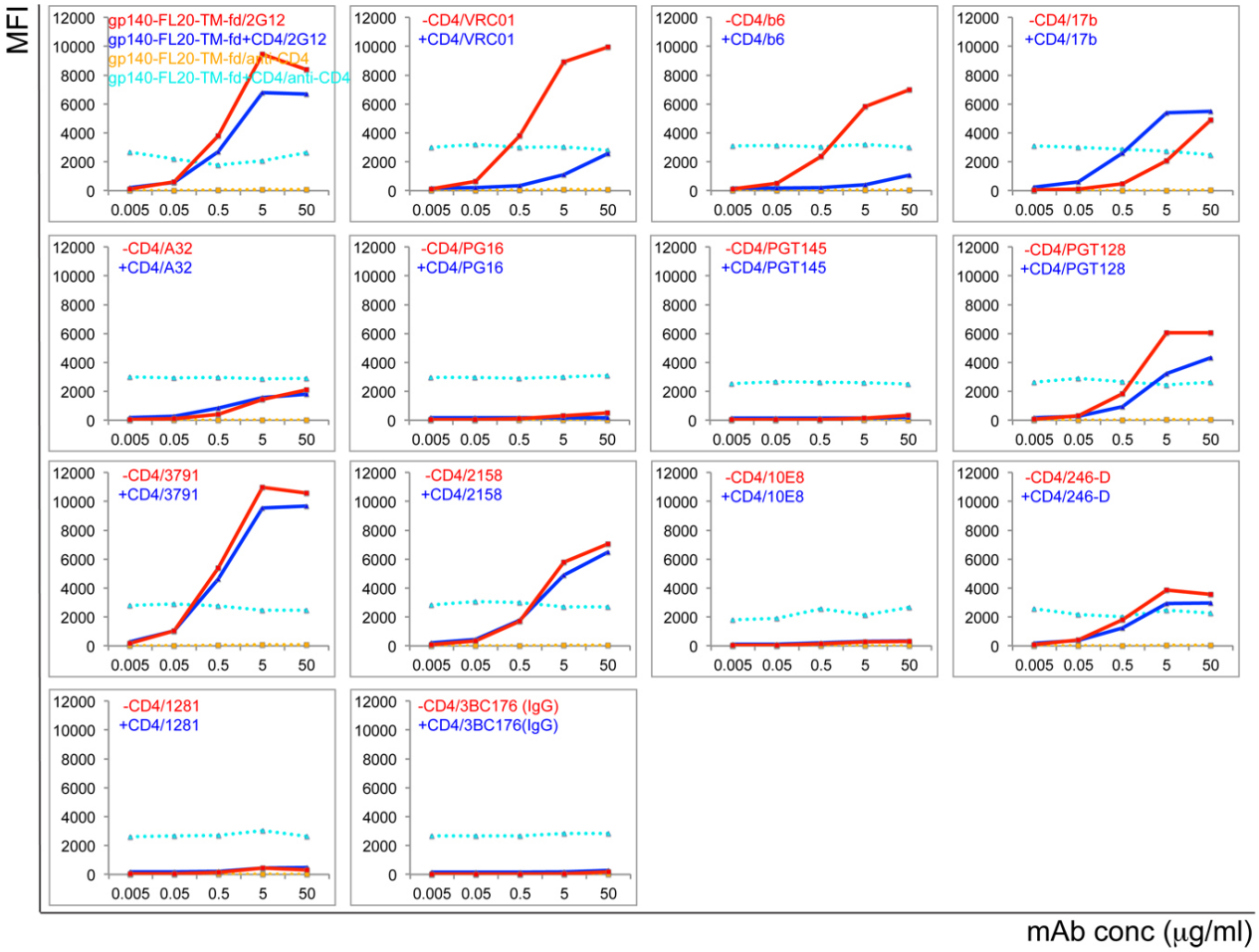
MFI
gp140-FL20-TM-fd/2G12
gp140-FL20-TM-fd+CD4/2G12
gp140-FL20-TM-fd/anti-CD4
gp140-FL20-TM-fd+CD4/anti-CD4
-CD4/VRC01
+CD4/VRC01
-CD4/b6
+CD4/b6
-CD4/17b
+CD4/17b
-CD4/A32
+CD4/A32
-CD4/PG16
+CD4/PG16
-CD4/PGT145
+CD4/PGT145
-CD4/PGT128
+CD4/PGT128
-CD4/3791
+CD4/3791
-CD4/2158
+CD4/2158
-CD4/10E8
+CD4/10E8
-CD4/246-D
+CD4/246-D
-CD4/1281
+CD4/1281
-CD4/3BC176 (IgG)
+CD4/3BC176(IgG)
0 2000 4000 6000 8000 10000 12000
0.005 0.05 0.5 5 50
mAb conc (μg/ml)

H (Fig. S19H)

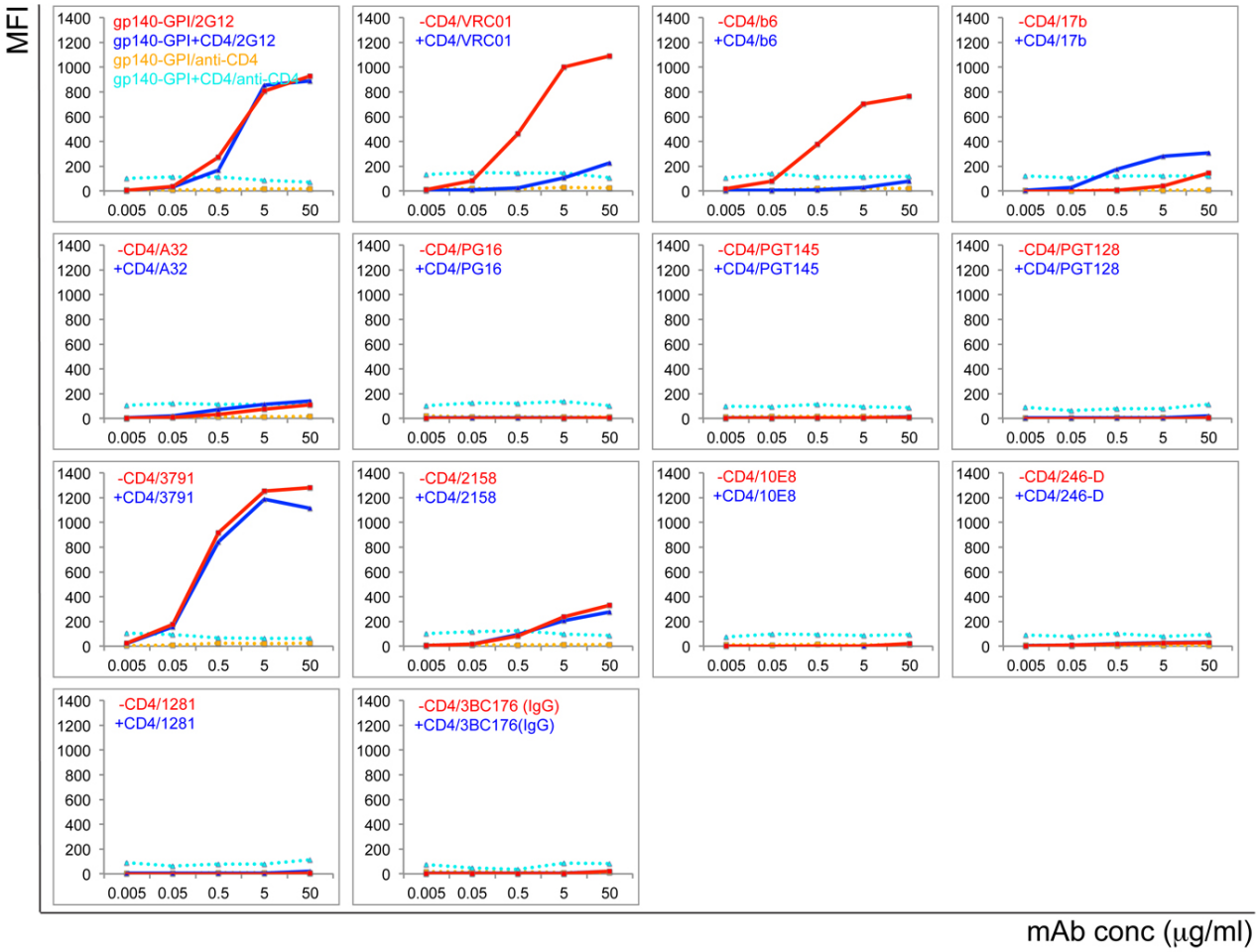

Fig. S19. Antigenic characteristics of the modified 92UG037.8 Env constructs presented on cell surfaces. (**A**) Plots of binding by selected antibodies to the Env trimer on the 92UG037.8 gp160-CT120 cell surfaces in the absence (red) or presence (blue) of soluble CD4. Fluorescent signal for bound CD4 is shown in the presence of CD4 (cyan) or in the absence of CD4 (orange). Unless specified, all antibodies used are Fab fragments. (**B**) Plots of binding by selected antibodies to the Env trimer on the 92UG037.8 gp160-CT90 cell surfaces. (**C**) Plots of binding by selected antibodies to the Env trimer on the 92UG037.8 gp160-CT60 cell surfaces. (**D**) Plots of binding by selected antibodies to the Env trimer on the 92UG037.8 gp160-CT30 cell surfaces. (**E**) Plots of binding by selected antibodies to the Env trimer on the 92UG037.8 gp140-TM-fd cell surfaces. (**F**) Plots of binding by selected antibodies to the Env trimer on the 92UG037.8

gp140-FL20-TM cell surfaces. (**G**) Plots of binding by selected antibodies to the Env trimer on the 92UG037.8 gp140-FL20-TM-fd cell surfaces. (**H**) Plots of binding by selected antibodies to the Env trimer on the 92UG037.8 gp140-GPI cell surfaces. Original flow cytometry histograms are shown in figs. S20-S27. The experiments were repeated at least two times with almost identical results.

Fig. S20.

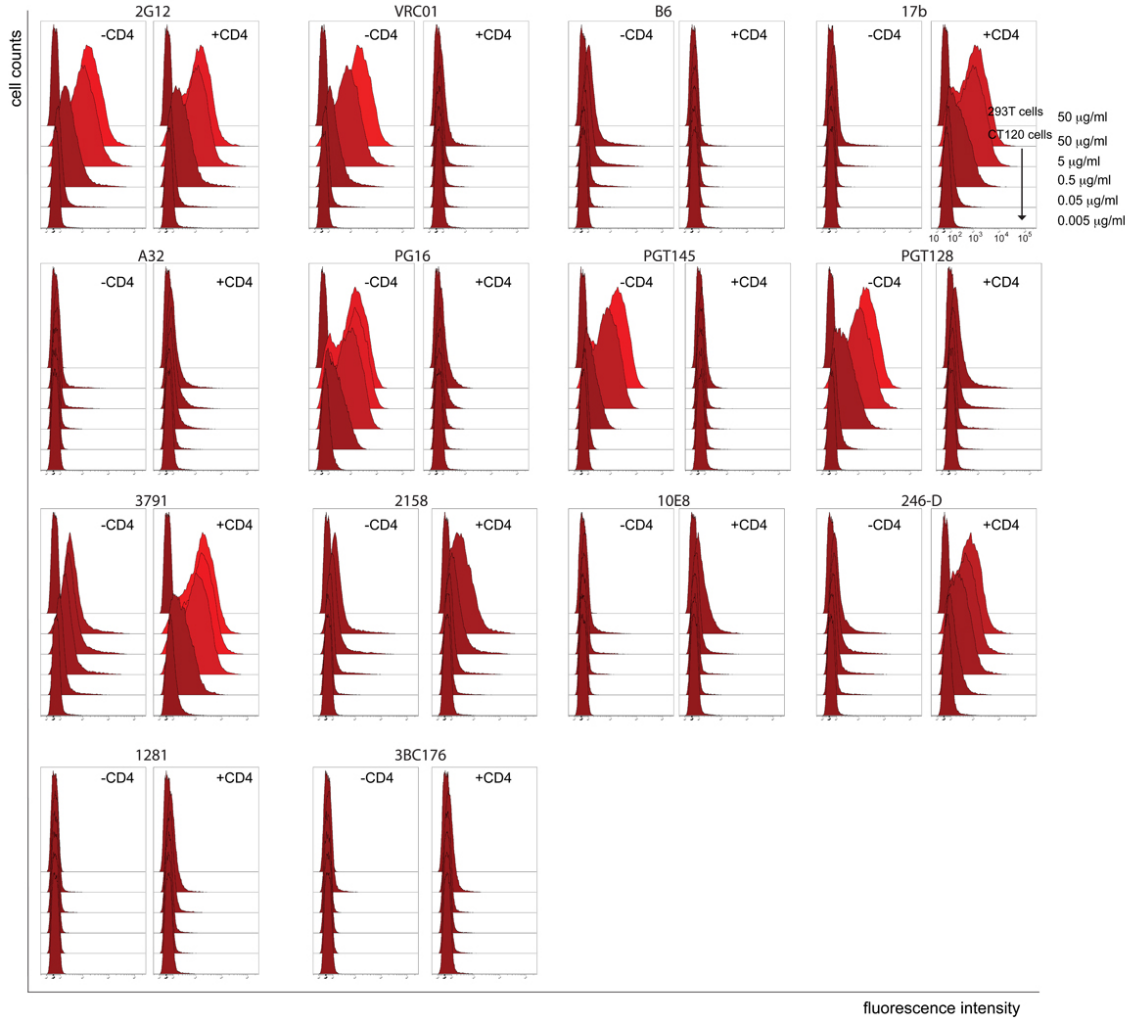

Fig. S20. Flow cytometry histograms of antibody binding to the Env trimer on the 92UG037.8 gp160-CT120 cell surfaces by a FACS assay. Data are summarized in Fig. S19A.

Fig. S21.

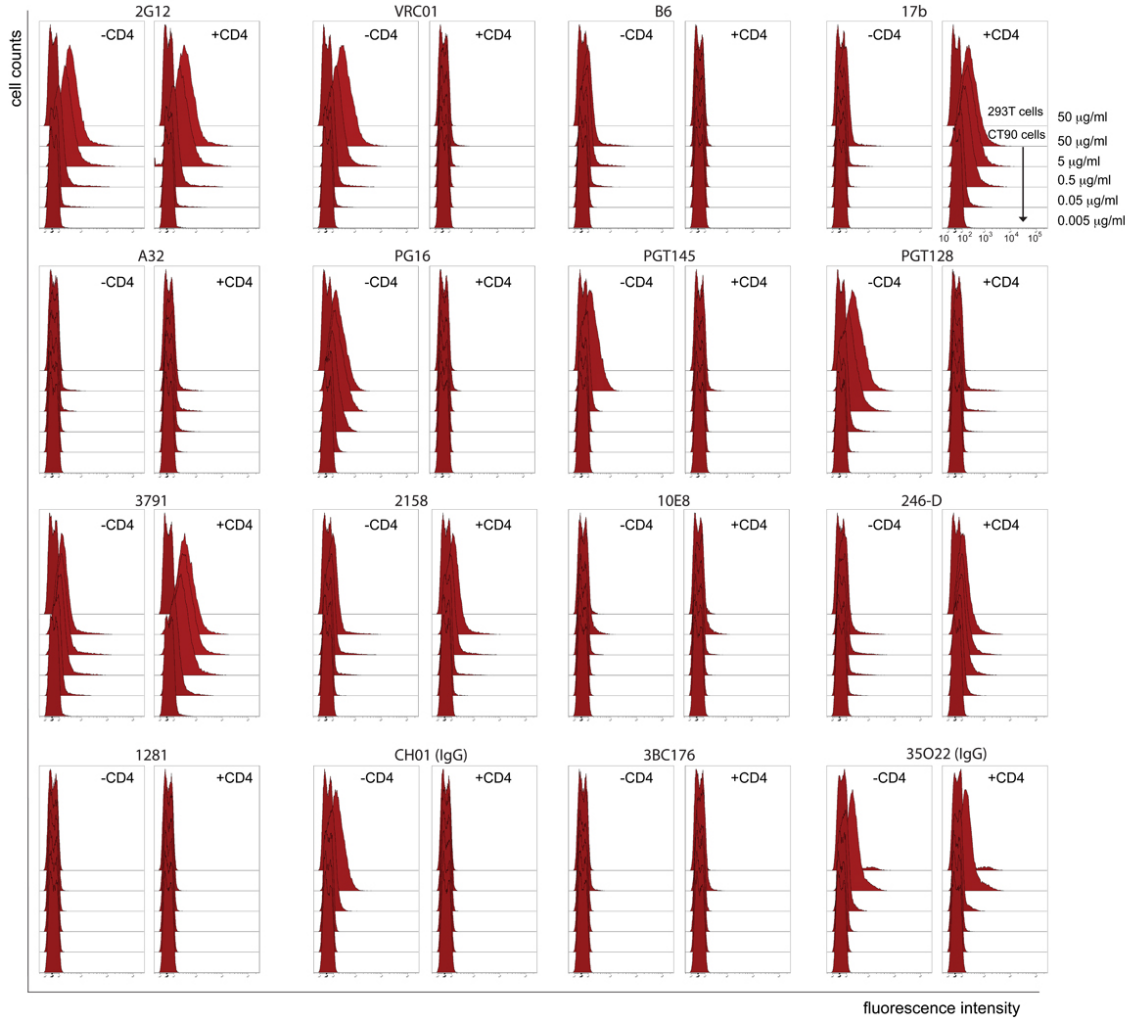

Fig. S21. Flow cytometry histograms of antibody binding to the Env trimer on the 92UG037.8 gp160-CT90 cell surfaces by a FACS assay. Data are summarized in fig. S19B.

Fig. S22.

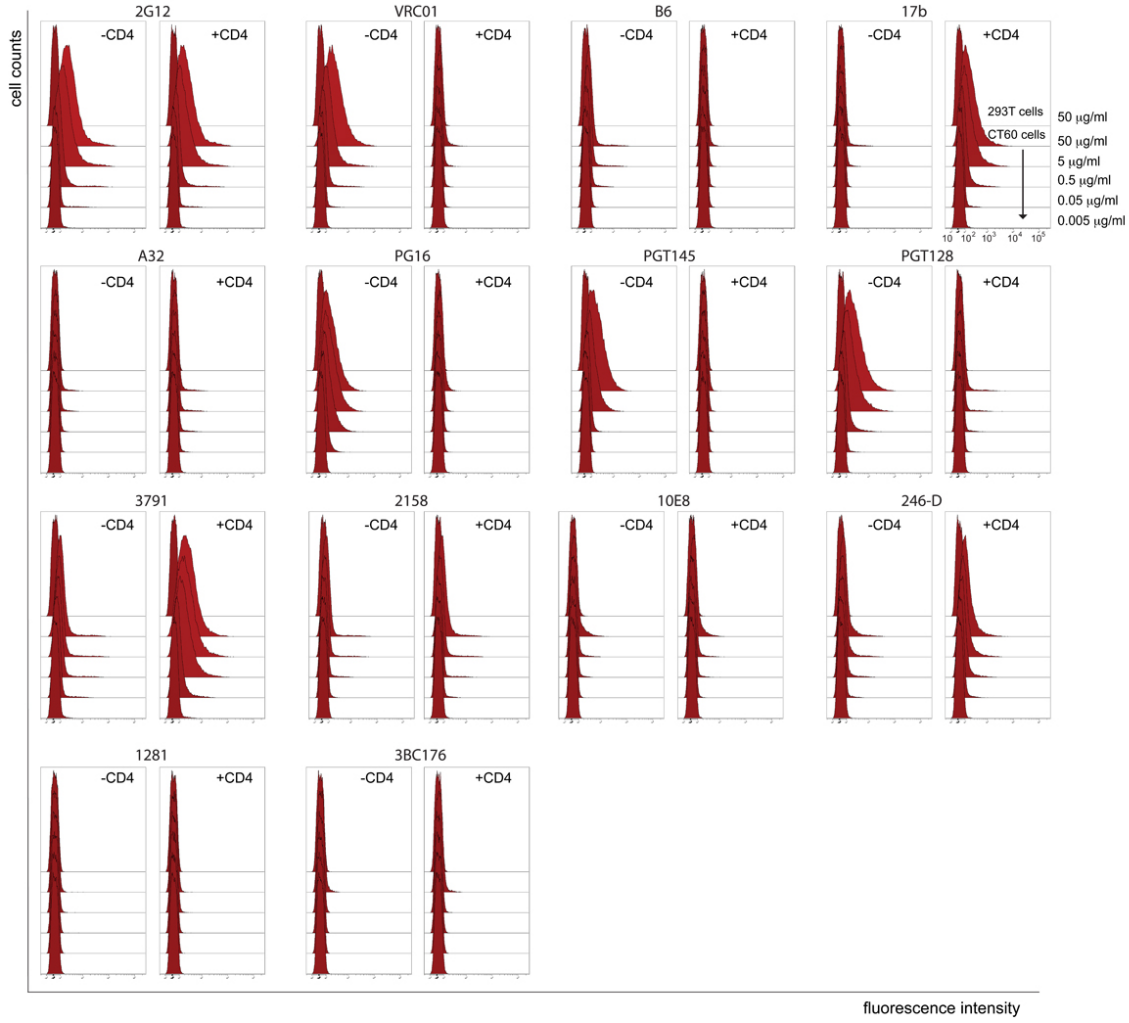

Fig. S22. Flow cytometry histograms of antibody binding to the Env trimer on the 92UG037.8 gp160-CT60 cell surfaces by a FACS assay. Data are summarized in fig. S19C.

Fig. S23.

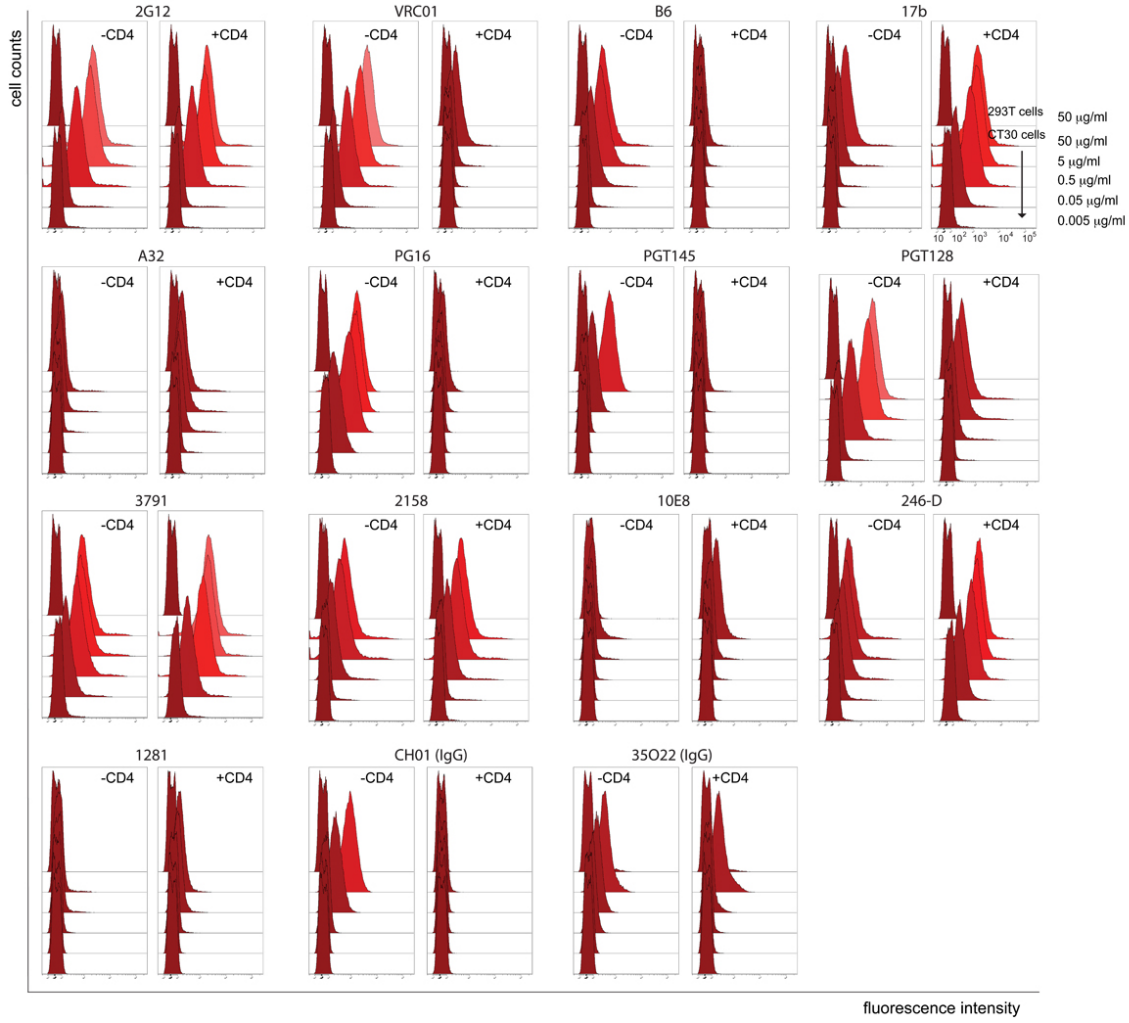

Fig. S23. Flow cytometry histograms of antibody binding to the Env trimer on the 92UG037.8 gp160-CT30 cell surfaces by a FACS assay. Data are summarized in fig. S19D.

Fig. S24.

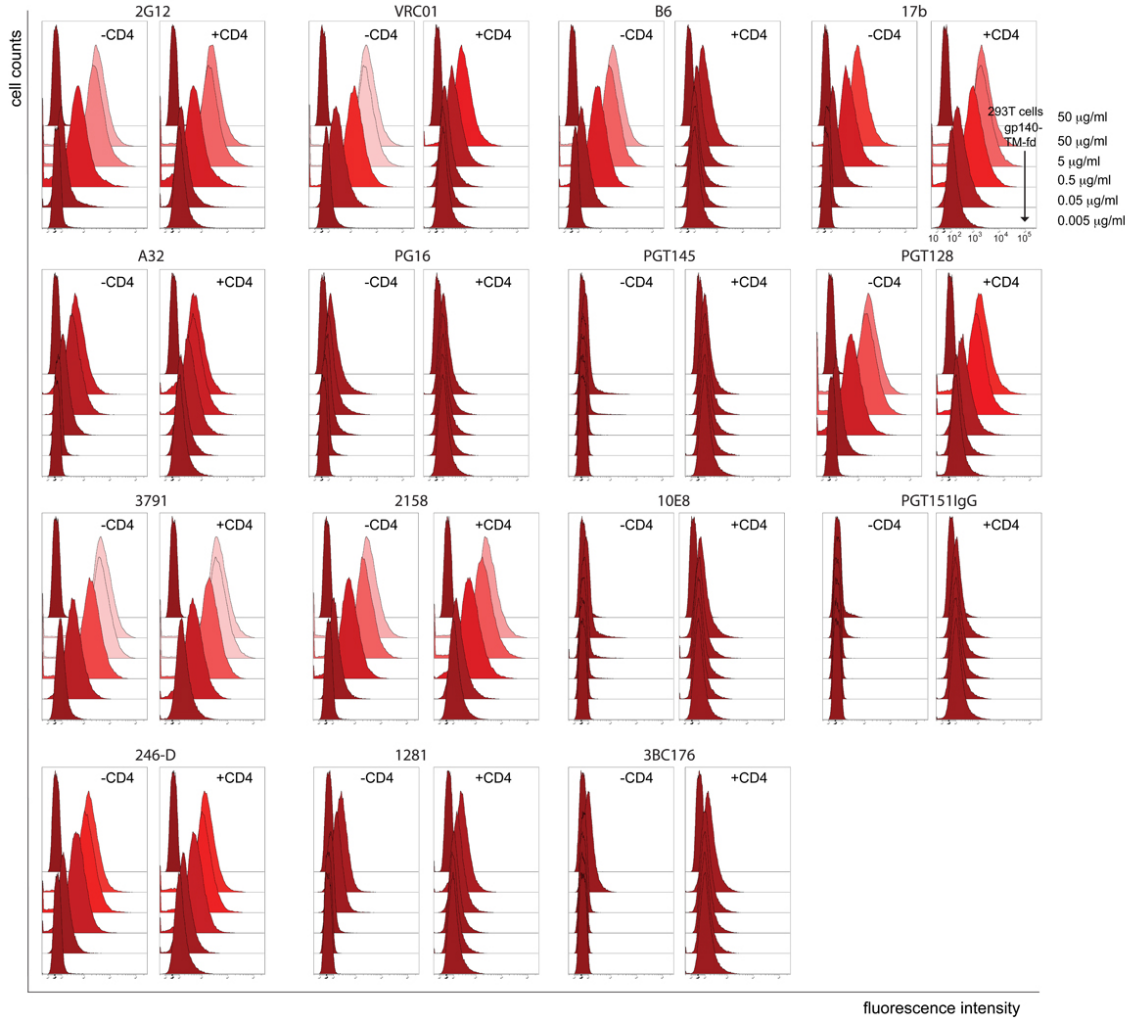

Fig. S24. Flow cytometry histograms of antibody binding to the Env trimer on the 92UG037.8 gp140-TM-fd cell surfaces by a FACS assay. Data are summarized in Fig. S19E.

Fig. S25.

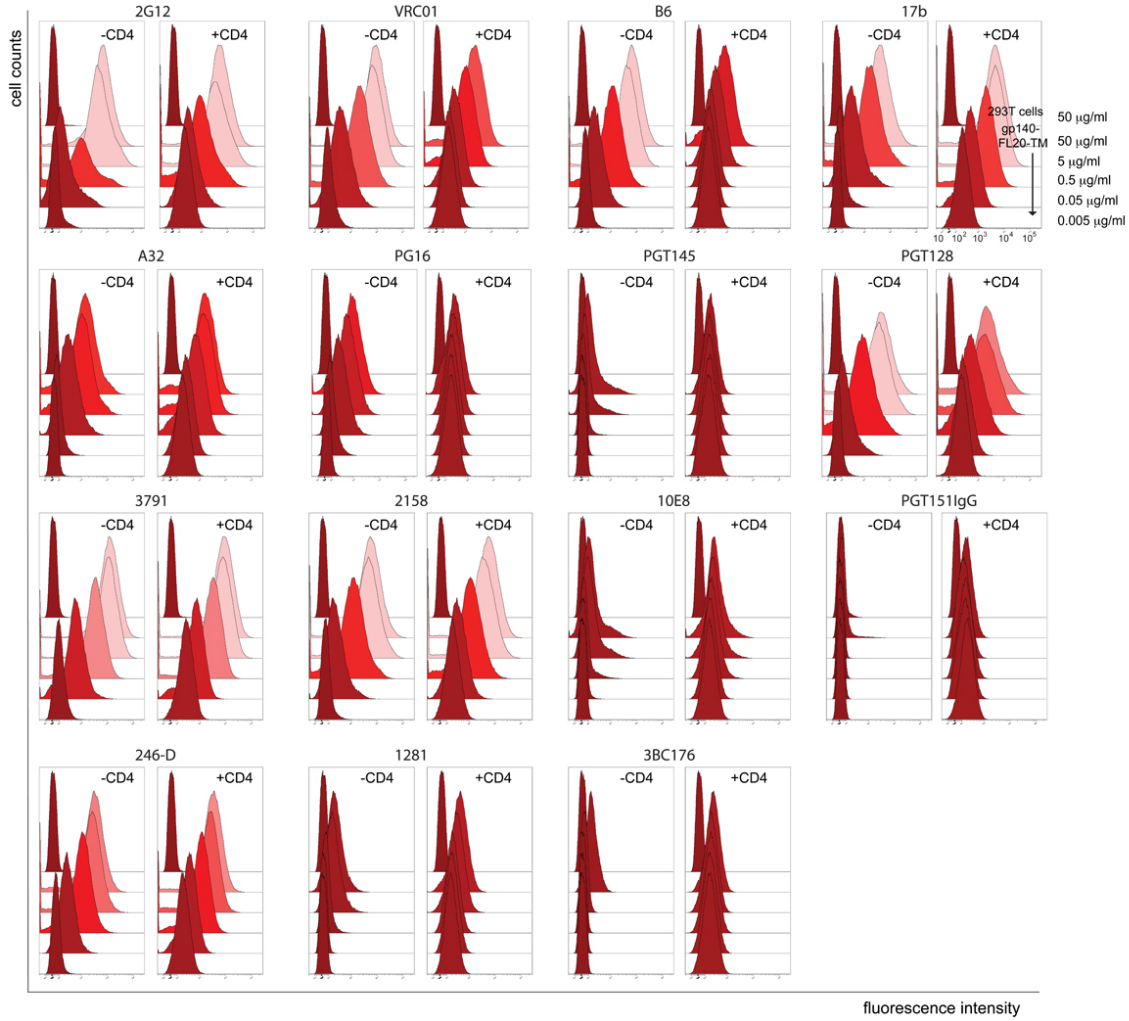

Fig. S25. Flow cytometry histograms of antibody binding to the Env trimer on the 92UG037.8 gp140-FL20-TM cell surfaces by a FACS assay. Data are summarized in fig. S19F.

Fig. S26.

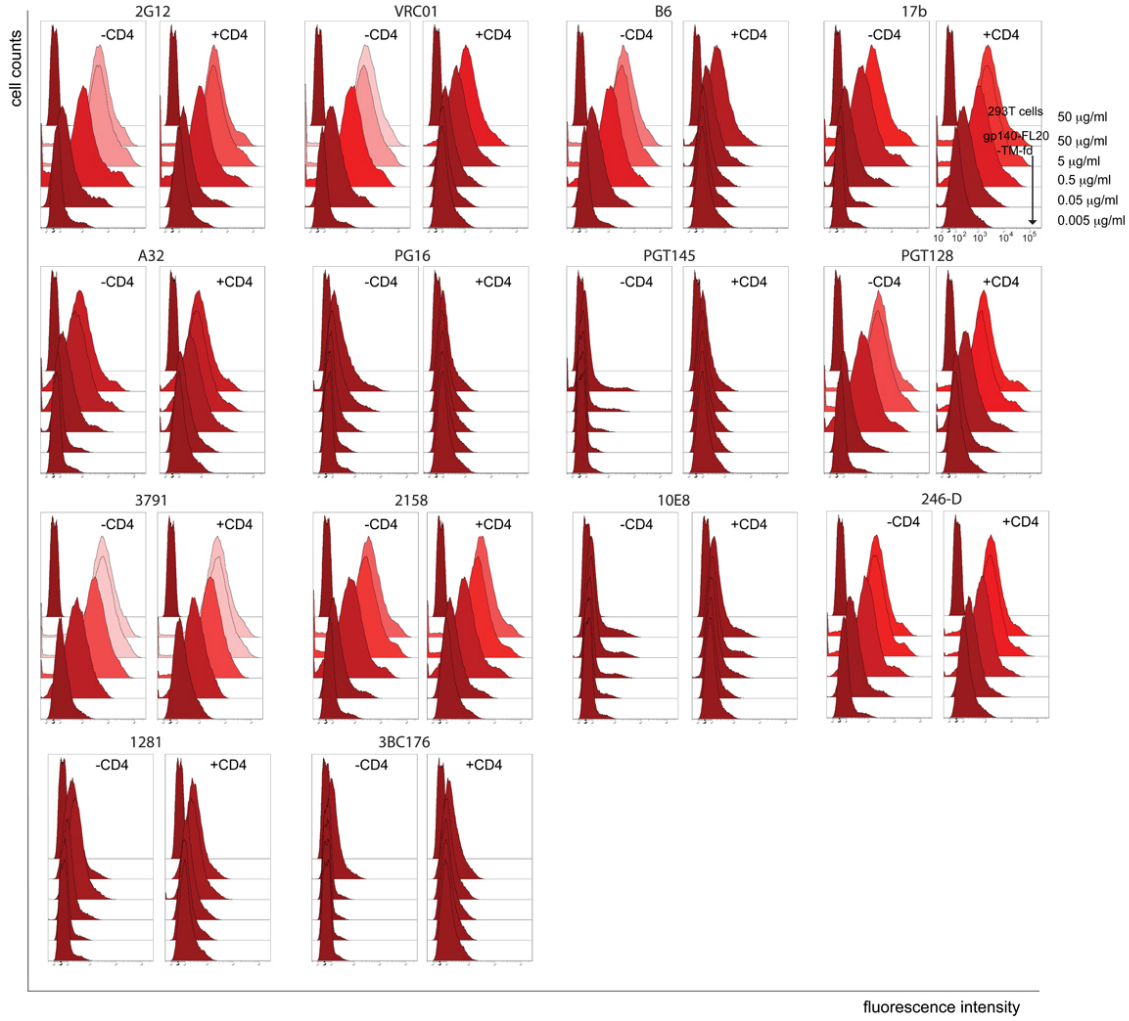

Fig. S26. Flow cytometry histograms of antibody binding to the Env trimer on the 92UG037.8 gp140-FL20-TM-fd cell surfaces by a FACS assay. Data are summarized in fig. S19G.

Fig. S27.

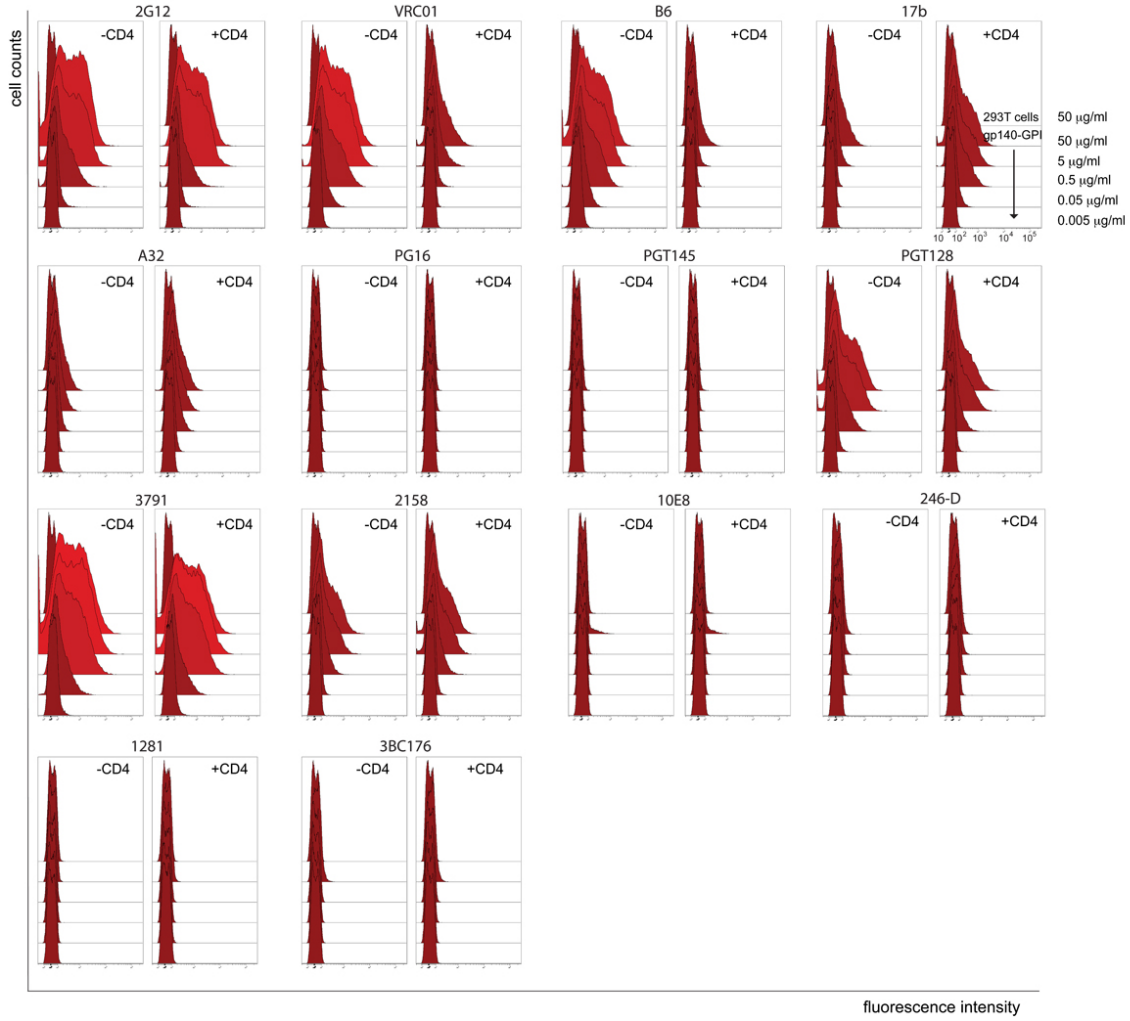

Fig. S27. Flow cytometry histograms of antibody binding to the Env trimer on the 92UG037.8 gp140-GPI cell surfaces by a FACS assay. Data are summarized in fig. S19H.

Fig. S28.

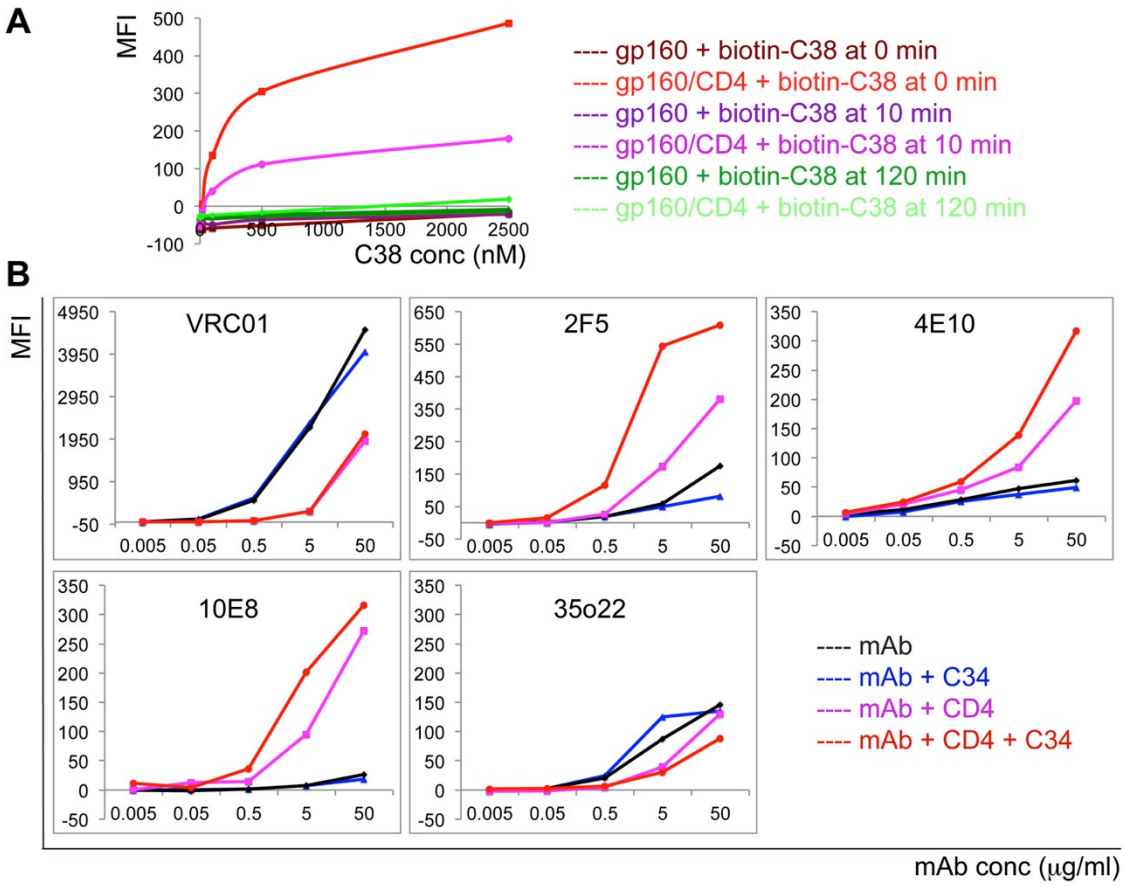

Fig. S28. MPER-directed bnAbs recognize a triggered Env trimer. (**A**) HR-2 derived peptide C38 binds the triggered Env trimers on the 92UG037.8 gp160 cell surfaces. The Env trimers were triggered by soluble CD4 at 37°C, which led to significant gp120 dissociation. Biotinylated peptide biotin-C38 was added to the cell surfaces at three different time point: 0 min, 10 min and 120 min. Biotin-C38 binding to the Env trimers was measured by FACS. (**B**) Antibodies, VRC01, 2F5, 4E10, 10E8 and 35O22, were incubated with the gp160 cells either alone or in the presence of another HR-2 derived peptide C34, or CD4, or both C34 and CD4. Antibody binding was detected by FACS. The experiments were repeated at least two times with almost identical results.

Table S1.

Table S1. List of monoclonal antibodies targeting HIV-1 Env used in this study.

Epitope	antibody	reference
CD4 binding site	VRC01, PGV04, NIH45-46, 12A12, 1NC9 and b6	ref (*48-53*)
N160 glycan dependent, trimer-specific epitope	PG9, PG16, CH01 and PGT145	ref (*54-56*)
N332 glycan dependent epitope	2G12, PGT128 and 10-1074	ref (*57-59*)
CD4i epitope	17b, A32 and 412d	ref (*60*, *61*)
V2	2158	ref (*62*)
V3	3791, 19b	ref (*63-65*)
MPER	2F5, 4E10 and 10E8	ref (*66-68*)
gp120-gp41 interface	PGT151/152, 8ANC195, 35O22	ref (*27*, *69-71*)
gp41 cluster I	240-D, 246-D and 7b2	ref (*72-75*)
gp41 cluster II	1281 and 167-D	ref (*72-75*)

Table S2.

Table S2. Summary of antigenic properties of gp160 and gp160ΔCT

Antibody			gp160 binding		gp160ΔCT binding	
epitope	name	Neut.[a]	-CD4	+CD4	-CD4	+CD4
CD4 bs	**VRC01**[b]	+	++++[c]	-	++++	-
	PGV04	+	++++	-	++++	-
	NIH45-46	+	++++	-	++++	-
	12A12	+	++++	-	++++	-
	b6	-	-	-	++	-
CD4i	17b	-	-	+++	+	+++
	412d	-	-	+++	-	++
	A32	-	-	-	-	-
V1V2-glycan	**PG9**	+	++++	-	++	-
	PG16	+	++++	-	++	-
	PGT145	+	+++++	-	++	-
V2	2158	-	-	+	++	++
V3	3791	-	-	++++	+++	++++
	19b	-	-	+++	++	++
V3-glycan	**PGT128**	+	++++	-	+++	+
	10-1074	+	++++	++	++++	++++
glycan	2G12	-	++	++	++++	++++
unknown	**3BC176**	+	-	-	-	-
MPER	**2F5**	+	-	-	-	-
	4E10	+	-	-	-	-
	10E8	+	-	-	-	+/-
cluster I	240-D	-	-	+++	+	++
	246-D	-	-	+++	+	++
	7b2	-	-	+++	+	++
cluster II	1281	-	-	-	-	-
	167-D	-	-	-	-	-
gp120-gp41	**35O22**	+	-	-	-	-
	PGT151	-	-	-	-	-
	8ANC195	+	+	-	+	+

[a]Neut., neutralization. [b]Antibodies highlighted in bold are bnAbs that neutralize the HIV-1 isolate 92UG037.8. [c]"+++++" and "++++" = strong binding; "+++" and "++" = moderate binding"; "+" = "weak binding" and "-" = no binding.

References and Notes

1. S. C. Harrison, Viral membrane fusion. *Nat. Struct. Mol. Biol.* **15**, 690–698 (2008). Medline doi:10.1038/nsmb.1456

2. D. C. Chan, D. Fass, J. M. Berger, P. S. Kim, Core structure of gp41 from the HIV envelope glycoprotein. *Cell* **89**, 263–273 (1997). Medline doi:10.1016/S0092-8674(00)80205-6

3. W. Weissenhorn, A. Dessen, S. C. Harrison, J. J. Skehel, D. C. Wiley, Atomic structure of the ectodomain from HIV-1 gp41. *Nature* **387**, 426–430 (1997). Medline doi:10.1038/387426a0

4. N. M. Flynn, D. N. Forthal, C. D. Harro, F. N. Judson, K. H. Mayer, M. F. Para; rgp120 HIV Vaccine Study Group, Placebo-controlled phase 3 trial of a recombinant glycoprotein 120 vaccine to prevent HIV-1 infection. *J. Infect. Dis.* **191**, 654–665 (2005). Medline doi:10.1086/428404

5. P. Pitisuttithum, P. Gilbert, M. Gurwith, W. Heyward, M. Martin, F. van Griensven, D. Hu, J. W. Tappero, K. Choopanya; Bangkok Vaccine Evaluation Group, Randomized, double-blind, placebo-controlled efficacy trial of a bivalent recombinant glycoprotein 120 HIV-1 vaccine among injection drug users in Bangkok, Thailand. *J. Infect. Dis.* **194**, 1661–1671 (2006). Medline doi:10.1086/508748

6. G. Frey, H. Peng, S. Rits-Volloch, M. Morelli, Y. Cheng, B. Chen, A fusion-intermediate state of HIV-1 gp41 targeted by broadly neutralizing antibodies. *Proc. Natl. Acad. Sci. U.S.A.* **105**, 3739–3744 (2008). Medline doi:10.1073/pnas.0800255105

7. By “triggered,” we mean any of the sequence of conformations that Env adopts after CD4 binding, on the pathway to fusion; by “native,” those with antigenic properties fully consistent with antibody neutralization.

8. T. Schiffner, Q. J. Sattentau, L. Dorrell, Development of prophylactic vaccines against HIV-1. *Retrovirology* **10**, 72 (2013). 10.1186/1742-4690-10-72 Medline

9. L. E. McCoy, R. A. Weiss, Neutralizing antibodies to HIV-1 induced by immunization. *J. Exp. Med.* **210**, 209–223 (2013). Medline doi:10.1084/jem.20121827

10. P. Liu, L. D. Williams, X. Shen, M. Bonsignori, N. A. Vandergrift, R. G. Overman, M. A. Moody, H. X. Liao, D. J. Stieh, K. L. McCotter, A. L. French, T. J. Hope, R. Shattock, B. F. Haynes, G. D. Tomaras, Capacity for infectious HIV-1 virion capture differs by envelope antibody specificity. *J. Virol.* **88**, 5165–5170 (2014). Medline doi:10.1128/JVI.03765-13

11. J. York, K. E. Follis, M. Trahey, P. N. Nyambi, S. Zolla-Pazner, J. H. Nunberg, Antibody binding and neutralization of primary and T-cell line-adapted isolates of human immunodeficiency virus type 1. *J. Virol.* **75**, 2741–2752 (2001). Medline doi:10.1128/JVI.75.6.2741-2752.2001

12. P. L. Moore, E. T. Crooks, L. Porter, P. Zhu, C. S. Cayanan, H. Grise, P. Corcoran, M. B. Zwick, M. Franti, L. Morris, K. H. Roux, D. R. Burton, J. M. Binley, Nature of nonfunctional envelope proteins on the surface of human immunodeficiency virus type 1. *J. Virol.* **80**, 2515–2528 (2006). Medline doi:10.1128/JVI.80.5.2515-2528.2006

13. T. Tong, E. T. Crooks, K. Osawa, J. M. Binley, HIV-1 virus-like particles bearing pure env trimers expose neutralizing epitopes but occlude nonneutralizing epitopes. *J. Virol.* **86**, 3574–3587 (2012). Medline doi:10.1128/JVI.06938-11

14. J. M. Kovacs, E. Noeldeke, H. J. Ha, H. Peng, S. Rits-Volloch, S. C. Harrison, B. Chen, Stable, uncleaved HIV-1 envelope glycoprotein gp140 forms a tightly folded trimer with a native-like structure. *Proc. Natl. Acad. Sci. U.S.A.* **111**, 18542–18547 (2014). Medline doi:10.1073/pnas.1422269112

15. R. W. Sanders, R. Derking, A. Cupo, J. P. Julien, A. Yasmeen, N. de Val, H. J. Kim, C. Blattner, A. T. de la Peña, J. Korzun, M. Golabek, K. de Los Reyes, T. J. Ketas, M. J. van Gils, C. R. King, I. A. Wilson, A. B. Ward, P. J. Klasse, J. P. Moore, A next-generation cleaved, soluble HIV-1 Env trimer, BG505 SOSIP.664 gp140, expresses multiple epitopes for broadly neutralizing but not non-neutralizing antibodies. *PLOS Pathog.* **9**, e1003618 (2013). Medline doi:10.1371/journal.ppat.1003618

16. J. Guenaga, N. de Val, K. Tran, Y. Feng, K. Satchwell, A. B. Ward, R. T. Wyatt, Well-ordered trimeric HIV-1 subtype B and C soluble spike mimetics generated by negative selection display native-like properties. *PLOS Pathog.* **11**, e1004570 (2015). Medline doi:10.1371/journal.ppat.1004570

17. J. B. Munro, J. Gorman, X. Ma, Z. Zhou, J. Arthos, D. R. Burton, W. C. Koff, J. R. Courter, A. B. Smith 3rd, P. D. Kwong, S. C. Blanchard, W. Mothes, Conformational dynamics of single HIV-1 envelope trimers on the surface of native virions. *Science* **346**, 759–763 (2014). Medline doi:10.1126/science.1254426

18. C. A. Bricault, J. M. Kovacs, J. P. Nkolola, K. Yusim, E. E. Giorgi, J. L. Shields, J. Perry, C. L. Lavine, A. Cheung, K. Ellingson-Strouss, C. Rademeyer, G. E. Gray, C. Williamson, L. Stamatatos, M. S. Seaman, B. T. Korber, B. Chen, D. H. Barouch, A multivalent clade C HIV-1 Env trimer cocktail elicits a higher magnitude of neutralizing antibodies than any individual component. *J. Virol.* **89**, 2507–2519 (2015). Medline doi:10.1128/JVI.03331-14

19. J. P. Nkolola, H. Peng, E. C. Settembre, M. Freeman, L. E. Grandpre, C. Devoy, D. M. Lynch, A. La Porte, N. L. Simmons, R. Bradley, D. C. Montefiori, M. S. Seaman, B. Chen, D. H. Barouch, Breadth of neutralizing antibodies elicited by stable, homogeneous clade A and clade C HIV-1 gp140 envelope trimers in guinea pigs. *J. Virol.* **84**, 3270–3279 (2010). Medline doi:10.1128/JVI.02252-09

20. J. M. Kovacs, J. P. Nkolola, H. Peng, A. Cheung, J. Perry, C. A. Miller, M. S. Seaman, D. H. Barouch, B. Chen, HIV-1 envelope trimer elicits more potent neutralizing antibody responses than monomeric gp120. *Proc. Natl. Acad. Sci. U.S.A.* **109**, 12111–12116 (2012). Medline doi:10.1073/pnas.1204533109

21. M. Pancera, T. Zhou, A. Druz, I. S. Georgiev, C. Soto, J. Gorman, J. Huang, P. Acharya, G. Y. Chuang, G. Ofek, G. B. Stewart-Jones, J. Stuckey, R. T. Bailer, M. G. Joyce, M. K. Louder, N. Tumba, Y. Yang, B. Zhang, M. S. Cohen, B. F. Haynes, J. R. Mascola, L. Morris, J. B. Munro, S. C. Blanchard, W. Mothes, M. Connors, P. D. Kwong, Structure and immune recognition of trimeric pre-fusion HIV-1 Env. *Nature* **514**, 455–461 (2014). Medline doi:10.1038/nature13808

22. P. Pugach, G. Ozorowski, A. Cupo, R. Ringe, A. Yasmeen, N. de Val, R. Derking, H. J. Kim, J. Korzun, M. Golabek, K. de Los Reyes, T. J. Ketas, J. P. Julien, D. R. Burton, I. A. Wilson, R. W. Sanders, P. J. Klasse, A. B. Ward, J. P. Moore, A native-like SOSIP.664 trimer based on an HIV-1 subtype B env gene. *J. Virol.* **89**, 3380–3395 (2015). Medline doi:10.1128/JVI.03473-14

23. E. J. Platt, K. Wehrly, S. E. Kuhmann, B. Chesebro, D. Kabat, Effects of CCR5 and CD4 cell surface concentrations on infections by macrophagetropic isolates of human immunodeficiency virus type 1. *J. Virol.* **72**, 2855–2864 (1998). Medline

24. In the FACS assay, bound primary antibodies were detected by a fluorescently labeled secondary antibody. Stably transfected cell lines for all Env constructs were necessary for obtaining high-quality data with mostly single sharp peaks in histograms; data that met these criteria gave reliable readings of MFI (mean fluorescence intensity) of a relatively homogeneous cell population (fig. S3C).

25. S. M. Alam, M. Morelli, S. M. Dennison, H. X. Liao, R. Zhang, S. M. Xia, S. Rits-Volloch, L. Sun, S. C. Harrison, B. F. Haynes, B. Chen, Role of HIV membrane in neutralization by two broadly neutralizing antibodies. *Proc. Natl. Acad. Sci. U.S.A.* **106**, 20234–20239 (2009). Medline doi:10.1073/pnas.0908713106

26. J. Chen, G. Frey, H. Peng, S. Rits-Volloch, J. Garrity, M. S. Seaman, B. Chen, Mechanism of HIV-1 neutralization by antibodies targeting a membrane-proximal region of gp41. *J. Virol.* **88**, 1249–1258 (2014). Medline doi:10.1128/JVI.02664-13

27. J. Huang, B. H. Kang, M. Pancera, J. H. Lee, T. Tong, Y. Feng, H. Imamichi, I. S. Georgiev, G. Y. Chuang, A. Druz, N. A. Doria-Rose, L. Laub, K. Sliepen, M. J. van Gils, A. T. de la Peña, R. Derking, P. J. Klasse, S. A. Migueles, R. T. Bailer, M. Alam, P. Pugach, B. F. Haynes, R. T. Wyatt, R. W. Sanders, J. M. Binley, A. B. Ward, J. R. Mascola, P. D. Kwong, M. Connors, Broad and potent HIV-1 neutralization by a human antibody that binds the gp41-gp120 interface. *Nature* **515**, 138–142 (2014). Medline doi:10.1038/nature13601

28. We obtained the same results regardless of whether we used a Fab or IgG form of the antibody or a 2-domain or 4-domain soluble CD4 (figs. S5A, S6, S5B, and S7). The antigenic properties of gp160 remained largely the same when the entire experiments were performed at 37°C, except that we saw significant CD4-induced gp120 shedding, as indicated by a lower level of 2G12, 17b ,and 3791 binding when CD4 was present and by an increase in 246-D binding (figs. S5C and S8).

29. C. C. LaBranche, M. M. Sauter, B. S. Haggarty, P. J. Vance, J. Romano, T. K. Hart, P. J. Bugelski, M. Marsh, J. A. Hoxie, A single amino acid change in the cytoplasmic domain of the simian immunodeficiency virus transmembrane molecule increases envelope glycoprotein expression on infected cells. *J. Virol.* **69**, 5217–5227 (1995). Medline

30. The modifications include replacing TM and CT with a GPI anchor (gp140-GPI), replacing CT with a foldon trimerization tag (gp140-TM-fd), inserting a flexible linker between gp120 and gp41 (gp140-FL20-TM), and adding both the foldon tag and the flexible linker (gp140-FL20-TM-fd).

31. T. G. Edwards, S. Wyss, J. D. Reeves, S. Zolla-Pazner, J. A. Hoxie, R. W. Doms, F. Baribaud, Truncation of the cytoplasmic domain induces exposure of conserved regions

in the ectodomain of human immunodeficiency virus type 1 envelope protein. *J. Virol.* **76**, 2683–2691 (2002). Medline doi:10.1128/JVI.76.6.2683-2691.2002

32. Y. Ye, Z. H. Si, J. P. Moore, J. Sodroski, Association of structural changes in the V2 and V3 loops of the gp120 envelope glycoprotein with acquisition of neutralization resistance in a simian-human immunodeficiency virus passaged in vivo. *J. Virol.* **74**, 11955–11962 (2000). Medline doi:10.1128/JVI.74.24.11955-11962.2000

33. T. Beaumont, A. van Nuenen, S. Broersen, W. A. Blattner, V. V. Lukashov, H. Schuitemaker, Reversal of human immunodeficiency virus type 1 IIIB to a neutralization-resistant phenotype in an accidentally infected laboratory worker with a progressive clinical course. *J. Virol.* **75**, 2246–2252 (2001). Medline doi:10.1128/JVI.75.5.2246-2252.2001

34. M. M. Freeman, M. S. Seaman, S. Rits-Volloch, X. Hong, C. Y. Kao, D. D. Ho, B. Chen, Crystal structure of HIV-1 primary receptor CD4 in complex with a potent antiviral antibody. *Structure* **18**, 1632–1641 (2010). Medline doi:10.1016/j.str.2010.09.017

35. M. Sarzotti-Kelsoe, R. T. Bailer, E. Turk, C. L. Lin, M. Bilska, K. M. Greene, H. Gao, C. A. Todd, D. A. Ozaki, M. S. Seaman, J. R. Mascola, D. C. Montefiori, Optimization and validation of the TZM-bl assay for standardized assessments of neutralizing antibodies against HIV-1. *J. Immunol. Methods* **409**, 131–146 (2014). Medline doi:10.1016/j.jim.2013.11.022

36. M. Li, F. Gao, J. R. Mascola, L. Stamatatos, V. R. Polonis, M. Koutsoukos, G. Voss, P. Goepfert, P. Gilbert, K. M. Greene, M. Bilska, D. L. Kothe, J. F. Salazar-Gonzalez, X. Wei, J. M. Decker, B. H. Hahn, D. C. Montefiori, Human immunodeficiency virus type 1 env clones from acute and early subtype B infections for standardized assessments of vaccine-elicited neutralizing antibodies. *J. Virol.* **79**, 10108–10125 (2005). Medline doi:10.1128/JVI.79.16.10108-10125.2005

37. M. Ferrer, S. C. Harrison, Peptide ligands to human immunodeficiency virus type 1 gp120 identified from phage display libraries. *J. Virol.* **73**, 5795–5802 (1999). Medline

38. G. Frey, S. Rits-Volloch, X. Q. Zhang, R. T. Schooley, B. Chen, S. C. Harrison, Small molecules that bind the inner core of gp41 and inhibit HIV envelope-mediated fusion. *Proc. Natl. Acad. Sci. U.S.A.* **103**, 13938–13943 (2006). Medline doi:10.1073/pnas.0601036103

39. N. Alsahafi, O. Debbeche, J. Sodroski, A. Finzi, Effects of the I559P gp41 change on the conformation and function of the human immunodeficiency virus (HIV-1) membrane envelope glycoprotein trimer. *PLOS ONE* **10**, e0122111 (2015). Medline doi:10.1371/journal.pone.0122111

40. C. Berlioz-Torrent, B. L. Shacklett, L. Erdtmann, L. Delamarre, I. Bouchaert, P. Sonigo, M. C. Dokhelar, R. Benarous, Interactions of the cytoplasmic domains of human and simian retroviral transmembrane proteins with components of the clathrin adaptor complexes modulate intracellular and cell surface expression of envelope glycoproteins. *J. Virol.* **73**, 1350–1361 (1999). Medline

41. J. F. Rowell, P. E. Stanhope, R. F. Siliciano, Endocytosis of endogenously synthesized HIV-1 envelope protein. Mechanism and role in processing for association with class II MHC. *J. Immunol.* **155**, 473–488 (1995). Medline

42. A. Bültmann, W. Muranyi, B. Seed, J. Haas, Identification of two sequences in the cytoplasmic tail of the human immunodeficiency virus type 1 envelope glycoprotein that inhibit cell surface expression. *J. Virol.* **75**, 5263–5276 (2001). Medline doi:10.1128/JVI.75.11.5263-5276.2001

43. E. Santos da Silva, M. Mulinge, D. Perez Bercoff, The frantic play of the concealed HIV envelope cytoplasmic tail. *Retrovirology* **10**, 54 (2013). 10.1186/1742-4690-10-54 Medline doi:10.1186/1742-4690-10-54

44. T. S. Postler, R. C. Desrosiers, The tale of the long tail: The cytoplasmic domain of HIV-1 gp41. *J. Virol.* **87**, 2–15 (2013). Medline doi:10.1128/JVI.02053-12

45. G. K. Lewis, Role of Fc-mediated antibody function in protective immunity against HIV-1. *Immunology* **142**, 46–57 (2014). Medline doi:10.1111/imm.12232

46. D. C. Chan, P. S. Kim, HIV entry and its inhibition. *Cell* **93**, 681–684 (1998). Medline doi:10.1016/S0092-8674(00)81430-0

47. L. V. Chernomordik, M. M. Kozlov, Mechanics of membrane fusion. *Nat. Struct. Mol. Biol.* **15**, 675–683 (2008). Medline doi:10.1038/nsmb.1455

48. X. Wu, Z. Y. Yang, Y. Li, C. M. Hogerkorp, W. R. Schief, M. S. Seaman, T. Zhou, S. D. Schmidt, L. Wu, L. Xu, N. S. Longo, K. McKee, S. O'Dell, M. K. Louder, D. L. Wycuff, Y. Feng, M. Nason, N. Doria-Rose, M. Connors, P. D. Kwong, M. Roederer, R. T. Wyatt, G. J. Nabel, J. R. Mascola, Rational design of envelope identifies broadly neutralizing human monoclonal antibodies to HIV-1. *Science* **329**, 856–861 (2010). Medline doi:10.1126/science.1187659

49. X. Wu, T. Zhou, J. Zhu, B. Zhang, I. Georgiev, C. Wang, X. Chen, N. S. Longo, M. Louder, K. McKee, S. O'Dell, S. Perfetto, S. D. Schmidt, W. Shi, L. Wu, Y. Yang, Z. Y. Yang, Z. Yang, Z. Zhang, M. Bonsignori, J. A. Crump, S. H. Kapiga, N. E. Sam, B. F. Haynes, M. Simek, D. R. Burton, W. C. Koff, N. A. Doria-Rose, M. Connors, J. C. Mullikin, G. J. Nabel, M. Roederer, L. Shapiro, P. D. Kwong, J. R. Mascola; NISC Comparative Sequencing Program, Focused evolution of HIV-1 neutralizing antibodies revealed by structures and deep sequencing. *Science* **333**, 1593–1602 (2011). Medline doi:10.1126/science.1207532

50. J. F. Scheid, H. Mouquet, B. Ueberheide, R. Diskin, F. Klein, T. Y. Oliveira, J. Pietzsch, D. Fenyo, A. Abadir, K. Velinzon, A. Hurley, S. Myung, F. Boulad, P. Poignard, D. R. Burton, F. Pereyra, D. D. Ho, B. D. Walker, M. S. Seaman, P. J. Bjorkman, B. T. Chait, M. C. Nussenzweig, Sequence and structural convergence of broad and potent HIV antibodies that mimic CD4 binding. *Science* **333**, 1633–1637 (2011). Medline doi:10.1126/science.1207227

51. E. Falkowska, A. Ramos, Y. Feng, T. Zhou, S. Moquin, L. M. Walker, X. Wu, M. S. Seaman, T. Wrin, P. D. Kwong, R. T. Wyatt, J. R. Mascola, P. Poignard, D. R. Burton, PGV04, an HIV-1 gp120 CD4 binding site antibody, is broad and potent in neutralization

but does not induce conformational changes characteristic of CD4. *J. Virol.* **86**, 4394–4403 (2012). Medline doi:10.1128/JVI.06973-11

52. D. R. Burton, A. J. Hessell, B. F. Keele, P. J. Klasse, T. A. Ketas, B. Moldt, D. C. Dunlop, P. Poignard, L. A. Doyle, L. Cavacini, R. S. Veazey, J. P. Moore, Limited or no protection by weakly or nonneutralizing antibodies against vaginal SHIV challenge of macaques compared with a strongly neutralizing antibody. *Proc. Natl. Acad. Sci. U.S.A.* **108**, 11181–11186 (2011). Medline doi:10.1073/pnas.1103012108

53. D. N. Sather, S. Carbonetti, J. Kehayia, Z. Kraft, I. Mikell, J. F. Scheid, F. Klein, L. Stamatatos, Broadly neutralizing antibodies developed by an HIV-positive elite neutralizer exact a replication fitness cost on the contemporaneous virus. *J. Virol.* **86**, 12676–12685 (2012). Medline doi:10.1128/JVI.01893-12

54. L. M. Walker, S. K. Phogat, P. Y. Chan-Hui, D. Wagner, P. Phung, J. L. Goss, T. Wrin, M. D. Simek, S. Fling, J. L. Mitcham, J. K. Lehrman, F. H. Priddy, O. A. Olsen, S. M. Frey, P. W. Hammond, S. Kaminsky, T. Zamb, M. Moyle, W. C. Koff, P. Poignard, D. R. Burton; Protocol G Principal Investigators, Broad and potent neutralizing antibodies from an African donor reveal a new HIV-1 vaccine target. *Science* **326**, 285–289 (2009). Medline doi:10.1126/science.1178746

55. L. M. Walker, M. Huber, K. J. Doores, E. Falkowska, R. Pejchal, J.-P. Julien, S.-K. Wang, A. Ramos, P.-Y. Chan-Hui, M. Moyle, J. L. Mitcham, P. W. Hammond, O. A. Olsen, P. Phung, S. Fling, C.-H. Wong, S. Phogat, T. Wrin, M. D. Simek, W. C. Koff, I. A. Wilson, D. R. Burton, P. Poignard; Protocol G Principal Investigators, Broad neutralization coverage of HIV by multiple highly potent antibodies. *Nature* **477**, 466–470 (2011). Medline doi:10.1038/nature10373

56. M. Bonsignori, D. C. Montefiori, X. Wu, X. Chen, K. K. Hwang, C. Y. Tsao, D. M. Kozink, R. J. Parks, G. D. Tomaras, J. A. Crump, S. H. Kapiga, N. E. Sam, P. D. Kwong, T. B. Kepler, H. X. Liao, J. R. Mascola, B. F. Haynes, Two distinct broadly neutralizing antibody specificities of different clonal lineages in a single HIV-1-infected donor: Implications for vaccine design. *J. Virol.* **86**, 4688–4692 (2012). Medline doi:10.1128/JVI.07163-11

57. A. Trkola, M. Purtscher, T. Muster, C. Ballaun, A. Buchacher, N. Sullivan, K. Srinivasan, J. Sodroski, J. P. Moore, H. Katinger, Human monoclonal antibody 2G12 defines a distinctive neutralization epitope on the gp120 glycoprotein of human immunodeficiency virus type 1. *J. Virol.* **70**, 1100–1108 (1996). Medline

58. R. Pejchal, K. J. Doores, L. M. Walker, R. Khayat, P. S. Huang, S. K. Wang, R. L. Stanfield, J. P. Julien, A. Ramos, M. Crispin, R. Depetris, U. Katpally, A. Marozsan, A. Cupo, S. Maloveste, Y. Liu, R. McBride, Y. Ito, R. W. Sanders, C. Ogohara, J. C. Paulson, T. Feizi, C. N. Scanlan, C. H. Wong, J. P. Moore, W. C. Olson, A. B. Ward, P. Poignard, W. R. Schief, D. R. Burton, I. A. Wilson, A potent and broad neutralizing antibody recognizes and penetrates the HIV glycan shield. *Science* **334**, 1097–1103 (2011). Medline doi:10.1126/science.1213256

59. H. Mouquet, L. Scharf, Z. Euler, Y. Liu, C. Eden, J. F. Scheid, A. Halper-Stromberg, P. N. Gnanapragasam, D. I. Spencer, M. S. Seaman, H. Schuitemaker, T. Feizi, M. C. Nussenzweig, P. J. Bjorkman, Complex-type N-glycan recognition by potent broadly

neutralizing HIV antibodies. *Proc. Natl. Acad. Sci. U.S.A.* **109**, E3268–E3277 (2012). Medline doi:10.1073/pnas.1217207109

60. M. Thali, J. P. Moore, C. Furman, M. Charles, D. D. Ho, J. Robinson, J. Sodroski, Characterization of conserved human immunodeficiency virus type 1 gp120 neutralization epitopes exposed upon gp120-CD4 binding. *J. Virol.* **67**, 3978–3988 (1993). Medline

61. R. Wyatt, J. Moore, M. Accola, E. Desjardin, J. Robinson, J. Sodroski, Involvement of the V1/V2 variable loop structure in the exposure of human immunodeficiency virus type 1 gp120 epitopes induced by receptor binding. *J. Virol.* **69**, 5723–5733 (1995). Medline

62. A. Pinter, W. J. Honnen, Y. He, M. K. Gorny, S. Zolla-Pazner, S. C. Kayman, The V1/V2 domain of gp120 is a global regulator of the sensitivity of primary human immunodeficiency virus type 1 isolates to neutralization by antibodies commonly induced upon infection. *J. Virol.* **78**, 5205–5215 (2004). Medline doi:10.1128/JVI.78.10.5205-5215.2004

63. J. Swetnam, E. Shmelkov, S. Zolla-Pazner, T. Cardozo, Comparative magnitude of cross-strain conservation of HIV variable loop neutralization epitopes. *PLOS ONE* **5**, e15994 (2010). 10.1371/journal.pone.0015994 Medline doi:10.1371/journal.pone.0015994

64. J. P. Moore, A. Trkola, B. Korber, L. J. Boots, J. A. Kessler 2nd, F. E. McCutchan, J. Mascola, D. D. Ho, J. Robinson, A. J. Conley, A human monoclonal antibody to a complex epitope in the V3 region of gp120 of human immunodeficiency virus type 1 has broad reactivity within and outside clade B. *J. Virol.* **69**, 122–130 (1995). Medline

65. C. F. Scott Jr., S. Silver, A. T. Profy, S. D. Putney, A. Langlois, K. Weinhold, J. E. Robinson, Human monoclonal antibody that recognizes the V3 region of human immunodeficiency virus gp120 and neutralizes the human T-lymphotropic virus type IIIMN strain. *Proc. Natl. Acad. Sci. U.S.A.* **87**, 8597–8601 (1990). Medline doi:10.1073/pnas.87.21.8597

66. J. Huang, G. Ofek, L. Laub, M. K. Louder, N. A. Doria-Rose, N. S. Longo, H. Imamichi, R. T. Bailer, B. Chakrabarti, S. K. Sharma, S. M. Alam, T. Wang, Y. Yang, B. Zhang, S. A. Migueles, R. Wyatt, B. F. Haynes, P. D. Kwong, J. R. Mascola, M. Connors, Broad and potent neutralization of HIV-1 by a gp41-specific human antibody. *Nature* **491**, 406–412 (2012). Medline doi:10.1038/nature11544

67. T. Muster, F. Steindl, M. Purtscher, A. Trkola, A. Klima, G. Himmler, F. Rüker, H. Katinger, A conserved neutralizing epitope on gp41 of human immunodeficiency virus type 1. *J. Virol.* **67**, 6642–6647 (1993). Medline

68. G. Stiegler, R. Kunert, M. Purtscher, S. Wolbank, R. Voglauer, F. Steindl, H. Katinger, A potent cross-clade neutralizing human monoclonal antibody against a novel epitope on gp41 of human immunodeficiency virus type 1. *AIDS Res. Hum. Retroviruses* **17**, 1757–1765 (2001). Medline doi:10.1089/08892220152741450

69. L. Scharf, J. F. Scheid, J. H. Lee, A. P. West Jr., C. Chen, H. Gao, P. N. Gnanapragasam, R. Mares, M. S. Seaman, A. B. Ward, M. C. Nussenzweig, P. J. Bjorkman, Antibody 8ANC195 reveals a site of broad vulnerability on the HIV-1 envelope spike. *Cell Reports* **7**, 785–795 (2014). Medline doi:10.1016/j.celrep.2014.04.001

70. C. Blattner, J. H. Lee, K. Sliepen, R. Derking, E. Falkowska, A. T. de la Peña, A. Cupo, J. P. Julien, M. van Gils, P. S. Lee, W. Peng, J. C. Paulson, P. Poignard, D. R. Burton, J. P. Moore, R. W. Sanders, I. A. Wilson, A. B. Ward, Structural delineation of a quaternary, cleavage-dependent epitope at the gp41-gp120 interface on intact HIV-1 Env trimers. *Immunity* **40**, 669–680 (2014). Medline doi:10.1016/j.immuni.2014.04.008

71. E. Falkowska, K. M. Le, A. Ramos, K. J. Doores, J. H. Lee, C. Blattner, A. Ramirez, R. Derking, M. J. van Gils, C. H. Liang, R. Mcbride, B. von Bredow, S. S. Shivatare, C. Y. Wu, P. Y. Chan-Hui, Y. Liu, T. Feizi, M. B. Zwick, W. C. Koff, M. S. Seaman, K. Swiderek, J. P. Moore, D. Evans, J. C. Paulson, C. H. Wong, A. B. Ward, I. A. Wilson, R. W. Sanders, P. Poignard, D. R. Burton, Broadly neutralizing HIV antibodies define a glycan-dependent epitope on the prefusion conformation of gp41 on cleaved envelope trimers. *Immunity* **40**, 657–668 (2014). Medline doi:10.1016/j.immuni.2014.04.009

72. J. Y. Xu, M. K. Gorny, T. Palker, S. Karwowska, S. Zolla-Pazner, Epitope mapping of two immunodominant domains of gp41, the transmembrane protein of human immunodeficiency virus type 1, using ten human monoclonal antibodies. *J. Virol.* **65**, 4832–4838 (1991). Medline

73. M. K. Gorny, S. Zolla-Pazner, Recognition by human monoclonal antibodies of free and complexed peptides representing the prefusogenic and fusogenic forms of human immunodeficiency virus type 1 gp41. *J. Virol.* **74**, 6186–6192 (2000). Medline doi:10.1128/JVI.74.13.6186-6192.2000

74. G. Frey, J. Chen, S. Rits-Volloch, M. M. Freeman, S. Zolla-Pazner, B. Chen, Distinct conformational states of HIV-1 gp41 are recognized by neutralizing and non-neutralizing antibodies. *Nat. Struct. Mol. Biol.* **17**, 1486–1491 (2010). Medline doi:10.1038/nsmb.1950

75. J. M. Binley, R. W. Sanders, B. Clas, N. Schuelke, A. Master, Y. Guo, F. Kajumo, D. J. Anselma, P. J. Maddon, W. C. Olson, J. P. Moore, A recombinant human immunodeficiency virus type 1 envelope glycoprotein complex stabilized by an intermolecular disulfide bond between the gp120 and gp41 subunits is an antigenic mimic of the trimeric virion-associated structure. *J. Virol.* **74**, 627–643 (2000). Medline doi:10.1128/JVI.74.2.627-643.2000